Use of gypsum and CKD to enhance early age strength of High Volume Fly Ash (HVFA) pastes

Bondar, D. and Coakley, E.

Original citation & hyperlink:
Bondar, D. and Coakley, E. (2014) Use of gypsum and CKD to enhance early age strength of High Volume Fly Ash (HVFA) pastes. Construction and Building Materials, volume 71 : 93-108.
http://dx.doi.org/10.1016/j.conbuildmat.2014.08.015

Use of Gypsum and CKD to enhance early age strength of High Volume Fly Ash (HVFA) pastes

Dali Bondar[1], Eoin Coakley[2]

[1]Research Assistant in Department of Civil Engineering, Architecture and Building, Coventry University, CV1 5FB, UK, Tel.: +44 024 7765 9022, E-mail addresses: dali.bondar@coventry.ac.uk, dlbondar@gmail.com

[2]Senior Lecturer in Department of Civil Engineering, Architecture and Building, Coventry University, CV1 5FB, UK

Abstract

Use of higher proportions of fly ash as a cement replacement in concrete has obvious environmental and performance benefits but high volumes of fly ash are not commonly used due to perceived lower early age strengths. In this investigation, addition of cement kiln dust (CKD) and gypsum to activate the fly ash was studied and the proportions used in the paste mixes were designed to optimize the mixture ingredients to achieve the highest early age compressive strength. Change of mineral phase composition and micro structure of the composites was analyzed. It was found that CKD was much more effective in activating the fly ash than gypsum. Appreciable early age compressive strengths were achieved for fly ash contents up to 60% of the binder and these observations were supported by analysis of the mineral phases.

Keywords: High Volume Fly Ash (HVFA) concrete; early age strength (EAS); cement kiln dust (CKD); gypsum; mineral phases

Introduction

The use of high volume fly ash (HVFA) concrete has gained increasing attention due to energy conservation, economic, and environmental considerations. Fly ash has become a commonly used constituent in concrete mixes because of its beneficial effects in several aspects including reduced water demand, improved fluidity during mixing and placing, improved dimensional stability, and increased long-term serviceability of concrete structures [1]. Fly ash particles are glassy and chemically stable because they are created at high temperatures, which means their reactivity during the hydration process

is low. At all replacement levels, fly ash generally slows down the setting time and hardening rate of concrete at early ages, especially under cold weather conditions. In a construction industry, heavily driven by reducing cost and duration of a project, increased concrete setting times are highly undesirable. More time has to be allowed before removal of formwork, which leads to delays and increased formwork costs. Also, any propping to in-situ cast members has to remain in position for longer.

Jiang and Malhotra investigated eight fly ashes from Canada and USA and reported that the 1 day compressive strength of concrete containing 55% replacement of Portland cement with fly ash, ranged from 6.3 – 13.9 MPa [2]. Atis found that compressive strengths of mixtures containing 70% class F fly ash or siliceous fly ash (class V in accordance with BS EN 197-1:2011) were consistently less than corresponding control mixes at all ages. However, the compressive strengths of mixtures containing 50% class F fly ash were comparable to the corresponding control mixes after 7 days [3]. Bouzoubaâ et al. investigated HVFA concrete using fly ash with Portland cement and concluded that it was possible to design concrete incorporating up to 50% replacement with fly ash that meets the strength requirements of the target compressive strengths (maximum of 14.7 MPa at 1 day). They observed the setting times of HVFA concrete mixes were 3 – 5 hours longer than those for control mixes but setting times were reduced by up to 40 min by increasing the fineness of fly ash [4, 5].

In a fly ash blended cement, the $Ca(OH)_2$ produced from hydration of cement acts as an activator for the fly ash, but low strengths of HVFA concretes at early ages indicates the need for an additional component to enhance the hydration ability, particularly of low calcium fly ash. Several studies have used sulphate activation and alkali activation to accelerate the pozzolanic reaction of fly ash. Gypsum and sodium sulphate have been used to study sulphate activation while NaOH, $Ca(OH)_2$ and other alkalis have been used to study alkali activation. X-ray diffraction and scanning electron microscopy confirmed that large amount of ettringite were formed in the early curing stages of fly ash cement pastes containing activators, resulting in a reduction in the pore size ranging from 0.01 – 5μm. Lee et al. found that for fly ash cement pastes with no activator, a small ettringite peak was observed at 9.1º (2θ) and over time the ettringite transferred to mono-sulfate and other products. XRD results supported the theory that large amounts of ettringite produced at early ages of hydration is likely to result in increased early strength of the fly ash concrete containing activators. In their study, SEM pictures of hydration products showed that in fly ash-cement pastes without activators, the hydrates were mostly C-S-H and mono-sulfate and the development of the microstructure was delayed due to pozzolanic activity. However, in pastes containing either Na_2SO_4 or K_2SO_4, SO_3^{2-} ions supplied by the activators, needle like hydration products (i.e., ettringite-

sized 1-5μm in diameter) were created. Other alkali compounds and crystallized mullite also appeared on the surface of Ca (OH) $_2$ [6]. Shi et al. studied the effect of sodium sulphate (Na_2SO_4) and calcium chloride ($CaCl_2$) on early microstructure development of lime fly ash pastes. X-ray analysis showed that addition of Na_2SO_4 resulted in the formation of substantial amounts of ettringite (Aft). Early age strengths increased with the dosage of sodium sulphate and this effect was much more significant for ash with higher CaO content due to higher proportion of reactive aluminates (3 – 5% addition of sodium sulphate resulted in strengths of 5 – 9 MPa after 1 day). Calcium chloride addition had a negligible effect on 1 day strengths with a maximum strength of 7 MPa for 5% addition of $CaCl_2$ when used with an ash of high CaO content [7, 8]. Bentz examined powder additions including aluminum trihydroxide, calcium hydroxide, condensed silica fume, limestone, and rapid-set cement. He reported that using an addition of either 5% calcium hydroxide or 10% rapid-set cement by mass of total cementitious materials accelerated the pozzolanic reaction significantly. Appreciable 3 day compressive strengths were recorded for both classes of fly ash for the material combinations examined in his study [9]. Supit and Shaikh studied the effect of nano-$CaCO_3$ on compressive strength development of mortars and concretes containing 40%-60% class F fly ash. The results showed that the addition of 1% nano-$CaCO_3$ increased the compressive strength although slightly reduced the workability of HVFA concretes [10].

Cement kiln dust (CKD) is a by-product of the Portland cement manufacturing process. Cement manufacturing plants generate approximately 30 million tonnes of CKD worldwide per year. All CKDs frequently contain alkalis (Na_2O and K_2O) and sulphates in much higher percentages than those found in Portland cement. The relatively high alkali content of CKD is the predominant factor preventing its recycling in cement manufacturing. However, its high alkali and sulphate content makes it an excellent activator for pozzolanic materials [11]. It contains free lime and varying amounts of alkalis, sulphates, and chlorides so caution is urged when selecting quantities of CKD to be used in blended cements to ensure durability issues do not arise. The Building Research Establishment (BRE) limits the alkali content of high alkali CEM 1-type component of a blended fly ash binder to <5.0 kg Na_2Oeq/m^3 for low, <3.0 kg Na_2Oeq/m^3 for normal, and <2.5 kg Na_2Oeq/m^3 for high reactivity aggregate [12]. The maximum chloride threshold for new construction is 0.15 – 0.25% by mass of cement but for existing buildings, it can be up to 0.4%. BS EN has removed the limit for maximum sulphate content in concrete to allow for slag type aggregates to be used, but 5% is seen as a notional maximum.

Little information on the suitability of CKD as an activator for fly ash is available. Bhatty studied binary, ternary and quaternary mixes using ordinary Portland cement, five different CKDs, two different types of fly ash (classes F and C), and blast furnace slag and observed that cements containing CKD alone had reduced strengths, setting times and workability's. The addition of fly ash to a CKD Portland cement system lowered the alkali content and resulted in improve strength [13, 14 & 15]. Maslehuddin et al. found that the compressive strength of fly ash concrete containing 10 – 20% fly ash and up to 10% CKD was marginally less than that of CEM 1 concrete [16]. He also observed that the initial and final setting times decreased when CKD was included in the mixes in his previous study [17]. Wang et al. studied the characteristics of a binder system consisting of 0 – 50% CKD and 0 – 75% slag replacement for Type 1 cement, with a total amount of supplementary cementitious materials less than or equal to 75%. It demonstrates that properly designed OPC-CKD-slag binders display properties comparable to pure OPC or an OPC-CKD blend. They also found that a CKD-slag specimen made without Portland cement also displays satisfactory compressive and flexural strength, which indicates that alkalis released from CKD may activate slag hydration [18]. Konsta-Gdoutos and Shah also confirmed that CKD can be successfully utilized to activate blast furnace slag and the rate of strength gain depends on the dissolution rate of slag, on the alkalinity of the reacting system and the existence of the optimum lime content [19]. Wang et al. also investigated the effects of activation methods on strength development of non-clinker cements made with 50% cement kiln dust and 50% Class F fly ash. These activation methods included ball mill co-grinding, chemical (NaOH addition), and elevated temperature curing. Particle size distribution, hydration products, and compressive strength of the binders were studied and soluble alkali and chloride content and pH value of the pastes were evaluated. The results indicated that all activation methods improved binder strength development and the strength improvement was more significant at early age than at later age. The major crystalline hydration product of the CKD-fly ash binders was ettringite and was found to be stable in the binder system for ages over 100 days. They also showed that curing at elevated temperatures is the most effective activation method for CKD-fly ash binder strength improvement. Grinding and NaOH addition usually reduced ettringite formation in CKD-fly ash system. It was reported that the CKD-fly ash pastes had much higher alkali and chloride contents but slightly lower pH value than the corresponding Portland cement paste [20, 21].

In this study, the intention is to use waste minerals to activate fly ash for use in in-situ cast HVFA concrete without considering grinding or use of elevated temperature curing which increases energy consumption in production. Cement kiln dust (CKD) and gypsum were added as activators to fly ash blended cement and the proportions used in the pastes were optimized to achieve a reasonable early age compressive strength while significantly reducing the proportion of cement within the blend. The overall

aim is to achieve the strength of a typical structural grade at 28 days without compromising on early age strength while achieving an appreciable reduction in consumption of cement within the mix. The micro structure of the cement products was characterized by scanning electron microscopy (SEM) while the phase changes and the percentage of reacted fly ash were analyzed by means of Fourier Transform Infrared Spectroscopy (FTIR), X-ray Fluorescence (XRF) and X-ray powder diffraction (XRD).

Materials and mix proportions

Two type of class F fly ash, Portland cement (CEM 1), cement kiln dust (CKD) and gypsum were used in this study. The mineralogical and chemical composition of the individual raw materials used was determined using X-ray diffraction (Figure 1) and X-ray fluorescence (Table 1). The only differences in mineral phase compositions of the investigated fly ashes was gypsum existed in fly ash 1 and identified crystalline major phases present in both samples were alumina silicate glass, quartz, mullite and magnetite. The main defined peaks on diffractograms related to quartz. High amounts of amorphous matter were present within the two investigated fly ash samples because of the background hump between 10 and 40 in the X-ray spectrum (Figure 1(a) & (b)). Identified crystalline major phases present in CEM 1 samples were: hatrurite, calcium aluminium oxide, millerite ferrian, quartz, anhydrite and dolomite (Figure 1(c)). In CKD, the main defined peaks correspond to quartz, calcite, portlandite, lime, anhydride, sylvite, and calcium aluminium oxide while for gypsum, gypsum, anhydride and calcite were present (Figure 1(d) & (e)). The density and the Blaine fineness of the binder materials were determined in accordance with BS EN 196-6 and these physical properties are presented in Table 2.

Thirteen HVFA cement pastes were prepared for both fly ash types to inform the optimization process. To ensure moderate early age strength is achieved, cement contents in excess of 20% (20%, 25% and 30% by mass) were used. CKD and gypsum contents used were 0%, 5% and 10% by mass as there were concerns over durability issues associated with higher contents. The remainder of the pastes was made up of fly ash at contents of 60%, 65% and 70% by mass. The proportions of the pastes are summarized in Table 3. The water to binder ratio of all mixes was kept constant at 0.3.

Experimental procedure

All the pastes were mixed in a laboratory HOBART mixer. For pastes with gypsum as one of the constituents, gypsum and fly ash was initially dry mixed and after adding half of the mixing water, mixing continued for 1 minute to attempt to dissolve the glass phase in fly ash. The other constituents (CKD, CEM 1, and the remaining water) were then subsequently added. For mixes that did not include gypsum, all powder materials were initially dry mixed and the water was subsequently added. From each paste, nine 50 mm cubes were cast to measure compressive strength. The specimens were cast in three layers and compacted with a tamping block. After casting, all the moulded specimens were covered with plastic sheeting and left in the casting room for 24 hours. They were then demoulded and the cubes were shrink-wrapped with plastic sheeting and kept in a moist curing container with water beneath the mesh that the samples were placed on. The samples were kept at approximately 20ºC and 90% relative humidity until required for testing. This curing regime was selected to ensure that no leaching occurred due to the presence of gypsum as an activator in some samples. For each sample, the compressive strength was determined on three cubes at 2, 7, and 28 days in accordance with BS EN 196.

Once paste samples were tested for compressive strength, pieces of the crushed samples were retained for microstructural and chemical analysis of the cementitious products. The microstructure of the cement products was characterized by scanning electron microscopy method (SEM) using a JOEL 6060LV Scanning Electron Microscope. Samples were hand ground with a mortar and pestle to be used for Fourier Transform Infrared Spectroscopy (FTIR). Samples for X-ray Fluorescence (XRF) and X-ray powder diffraction (XRD) were ground with a planetary mill. FTIR was carried out using a Perkin Elmer Spectrum 100 FT-IR Spectrometer with an ATR attachment, XRF analysis was carried out using a PAN analytical Axios Advanced XRF spectrometer and XRD patterns were obtained using a Bruker D8 Advance with DaVinci, which was equipped with a LynxEye Linear Position Sensitive Detector and a 90-position autosampler diffractometer, using a Cu K-alpha radiation tube.

Results and discussion

Figure 2 shows 2 day, 7 day and 28 day compressive strengths (average of 3 samples) for each binder proportion for both types of class F fly ash. The emphasis in this investigation is primarily on early age (2 day) strength. The highest early age compressive strength (11.11 MPa for fly ash 1 and 16.36 MPa for fly

ash 2) were both related to mix No. 10 (60% Fly Ash + 30% CEM 1 + 10% CKD). All mixes that used gypsum only to activate the fly ash achieved lower 2 day strengths than the corresponding control paste (No. 1) and in some cases, reductions in strength of the order of 50% were observed. For fly ash 1, any pastes that included gypsum were weaker than the control paste after 2 days. For fly ash 2 however, two mixes that included 5% gypsum in conjunction with 5 – 10% CKD were 10 – 20% stronger than the corresponding control paste. This moderate increase in strength is attributed to the contribution of the CKD to activation of the fly ash. Generally, it was observed that use of CKD and gypsum together for activating fly ash gave lower early age strength than when CKD was used alone. Poon et al. found that gypsum is less effective in activating fly ash at room temperature and that it leads to significantly greater strength enhancements at elevated curing temperatures [22]. Therefore, use of gypsum to activate fly ash is more applicable to the precast concrete industry where heated curing is regularly used.

Generally, mixes that used CKD only to activate the fly ashes led to increases in early age strength relative to the control pastes. Only mix No. 4 for fly ash 1 led to a decrease in strength but this mix had only 20% CEM 1 (as opposed to 30% in the control paste). 60% Fly Ash + 30% CEM 1 + 10% CKD achieved increases in 2 day strength of 45% and 184% (relative to the corresponding control paste) for fly ash 1 and fly ash 2 respectively. These substantial increases in strength were achieved by replacing 10% of fly ash (relative to the total binder content) with CKD. This strength enhancement at early age is attributed to the high total equivalent alkalis increasing the rate of reaction between the aluminates and the calcium oxide.

For fly ash 1, pastes with various proportions of waste activators generally showed lower strength than the control paste (No. 1) at 28 days. However, the proportion of highest strength (No. 10), showed 15% higher compressive strength at 28 days (23.63 MPa for Mix No. 1 and 27.11 MPa for Mix No. 10). For fly ash 2, pastes with waste activators generally showed higher 28 day strength than the control paste (No. 1) and the proportion of highest strength (No. 10) showed 61% higher compressive strength at 28 days (17.58 MPa for Mix No. 1 and 28.28 MPa for Mix No. 10). Although the 2 day strength of mixes that included gypsum was relatively low, the strength gain up to 28 days was more significant. Therefore, if early age strength is not critical, use of CKD and gypsum together can be effective in achieving acceptable 28 day strengths in HVFA pastes.

The control paste for fly ash 1 generally achieved higher compressive strengths than that for fly ash 2 (7.68 MPa compared to 5.76 MPa at 2 days and 23.63 MPa compared to 17.58 MPa at 28 days). This is attributed to the higher CaO content of fly ash 1, which is 1.61% higher than for fly ash 2.

The consistence and setting times of the control pastes and the pastes of highest strength was determined in accordance with BS EN 196-3 and results are shown in Table 4a & 4b. The pastes of highest strength had shorter initial and final setting times than the equivalent control pastes. Reductions in initial setting time relative to the corresponding control pastes were 32% for both fly ash 1 and fly ash 2 (without superplasticiser). This represents a substantial reduction in setting time due to the inclusion of 10% of CKD within the binder.

As mentioned previously, CKD tends to contain higher amounts of alkalis and sulphates than CEM 1. Consequently, adding excessive amounts of CKD to the binder could lead to durability issues. CKD has been shown to significantly improve early age strength of HVFA mixes due to the high alkali content but caution is urged to ensure no detrimental effects on long-term durability. In the paste of highest strength (No. 10) that included 60% Fly Ash + 30% CEM 1 + 10% CKD, the alkali content of CEM 1 and CKD (i.e. CEM 1-type content of the binder) is calculated as 0.6% (alkali in CEM 1 = 0.225% and in CKD = 0.378%) from the chemical compositions of the binder materials given in Table 1. This is therefore classified as a low alkali binder according to BRE (2004) [12]. However, XRF analysis of the cementitious products for the pastes of highest strength (No. 10) showed 1.45% and 1.91% alkalis ($\%Na_2Oeq = \%Na_2O + 0.658\% K_2O$) for fly ash 1 and fly ash 2 respectively. These are a little bit less than the observed alkalis in the weighted sum of the raw materials (2.00 and 2.39 for fly ash 1 and fly ash 2 respectively), which may be due to the leaching of alkali. Since the Na and K are not present in the XRD minerals, they may exist in solid solution in the phases already identified, they may be present in phases below the detection limit for those samples, or they may be amorphous or only partly crystalline. These alkalis, which are not crystalline, seem to be active and a further detailed study of the potential for alkali aggregate reaction of this blended cement is suggested. The proportion of sulphates in the pastes of highest strength (No. 10) was also calculated from Table 1 as 1.59% for fly ash 1 and 1.42% for fly ash 2, which is less than the notional maximum of 5%. However, XRF analysis of the cementitious products for these mixes showed the percentages of sulphates of 2.17% for fly ash 1 and 2.64% for fly ash 2. The observed increase in the sulphates in the products (relative to the total in the raw materials) may be due to a lack of homogeneity in the test powder samples or sulphates in the mix water.

Statistical analysis of 2-day strength results

An analysis of the Signal to Noise (S/N) ratio was used to evaluate the experimental results and confirm the optimized amount of each constituent in the binder based on Taguchi methods. Philosophy of the Taguchi method is to achieve best results by minimizing the deviation from a target. The product should be designed so that it is immune to uncontrollable environmental factors. In other words, the signal (product quality) to noise (uncontrollable factors) ratio should be high. This method optimizes the target based on the levels selected and not for the whole domain. Three types of S/N ratio analysis are available: (1) Lower is Better (LB), (2) Nominal is Better (NB) and (3) Higher is Better (HB). Since the highest early age compressive strength is targeted in this study, the S/N ratio with HB characteristic was applied, and this is defined by Eq. (1):

$$S/N = -10\log\left(1/n \sum_{i=1}^{n} 1/Y_i^2\right) \qquad (1)$$

where (i = 1 to n) and n is the number of repetitions under the same experimental conditions and Y represents the 2 day compressive strength of the paste samples. To determine the optimum conditions, the analysis of variance (ANOVA) statistical approach was adopted. The values of the S/N ratio were substituted into Eq. (2) and the mean of the S/N ratios of a certain factor in the ith level, is calculated.

$$(M)_{Factor=I}^{Level=i} = 1/n_{Ii} \sum_{j=1}^{n} [(S/N)_{Factor=I}^{Level=i}]_j \qquad (2)$$

In Eq. (2), n_{Ii} represents the appearance of factor I in the level i, and $[(S/N)_{Factor=I}^{Level=i}]_j$ is the S/N ratio of factor I in the level i, and its appearance sequence is the jth. Using this process, the mean of the S/N ratios of the other factors in a certain level was determined. From this, the S/N response table was obtained and the optimum conditions were established [23].

Table 5a & 5b show the S/N ratio of each design calculated according to Eq. (1) and values in bold refer to the maximum value of S/N ratio among the 13 mixes (No. 10). These values of the S/N ratio were substituted into Eq. (2) and the mean of the S/N ratios of a certain factor in the ith level, $(M)_{Factor=I}^{Level=i}$, was obtained (Table 6a & 6b). M_4 denotes the mean of the lowest 4 S/N ratios for a particular factor and M_5 denotes the mean of 5 S/N ratios where applicable within the test programme. The values in **bold** in

Table 6a & 6b refer to the maximum value of the mean of the S/N ratios of a certain factor among three levels, which indicate the optimum conditions for the early age compressive strength. Therefore, 30% CEM 1, 10% CKD and 0% gypsum were generally found to be the optimum proportions to obtain the highest early age strength.

The Response Surface Method was also used to check the optimization of paste proportioning. The analysis was carried out using Surfer 8 software and double checked with MINITAB 16 software, which use a quadratic model for prediction of results considering the interaction of effects between components within a specified domain. The material proportions and early age compressive strength of the thirteen pastes were analyzed for both fly ash types.

The output from Surfer 8 gives contour plots of the various activators (CEM 1, CKD and gypsum) vs. fly ash shown in Figures 3 & 4. Contour plots from Minitab have the benefit of plotting the effect of three binder constituents together and results are shown in Figures 5 & 6. Both sets of results show that 60% Fly Ash + 30% CEM 1 + 10% CKD has been confirmed as the optimum proportion to maximize the early age compressive strength for both types of class F fly ash. Surfer 8 output shows that for fly ash replacement level up to 67%, early age strength increases with increasing CKD content (Figure 3b & 4b), when considering a maximum limit on CKD content of 10%. To improve early strengths, gypsum by itself was not particularly helpful for curing at room temperature (Figure 3c & 4c).

Microstructure investigation from Scanning Electronic Microscopy (SEM) and Fourier transforms infrared spectroscopy (FTIR)

Figures 7a – 7h show the micro-structural characteristics from SEM imaging of selected pastes. Unreacted fly ash particles can be readily identified in images as spherical particles and this allows the degree of fly ash activation to be visually assessed. Images show that increasing the amount of CKD up to 10% reduces the amount of remaining unreacted fly ash (by comparing Figure 7a to 7c and Figure 7e to 7g). The optimum binder for fly ash 2 shows less unreacted fly ash particles than the optimum binder for fly ash 1 (from Figures 7g & 7c respectively), which correlates with the increased strength gain (relative to the respective control mix). Inclusion of 10% CKD increased dissolution of the fly ash particles and produced a denser uniform microstructure compared to the

higher gel porosity of the respective control mixes. Figures 7d & 7h show the microstructure of pastes that used gypsum for fly ash activation and in both cases; ettringite (AFt) formation (identified by needle-like hydration products) was relatively low. However, gel porosity appears relatively low for both pastes and moderate strength gain was observed up to 28 days.

The FTIR spectra of pastes are shown in Figure 8. A broad transmission around 3400 cm^{-1} corresponded to calcium silicate hydrate (C-S-H). In addition, calcite ($CaCO_3$) with C-O stretching vibration around 875-700 cm^{-1} and around 1420-1410 cm^{-1} was found in all of the mixes. Wave numbers around 650-1800 cm^{-1} represent phase transformation. Si-O stretching vibration peaks around 970-960 cm^{-1} of C-S-H, K-C-S-H and NA-C-S-H compounds were found. The other phase observed in the samples was around 1500-1400 cm^{-1} and 870 cm^{-1} corresponding to C-O vibration of CO_3^{-2} in $CaCO_3$. The spectrum for samples made of optimum mix proportion (60% Fly Ash + 30% CEM 1 + 10% CKD) contained one peak at 3381 cm^{-1} and 3405 cm^{-1} for fly ash 1 and fly ash 2, respectively which display calcium silicate hydrate (C-S-H) stretching bands. However, for samples made of control mix proportion (70% Fly Ash + 30% CEM 1), this is not appearing as a sharp peak. At mixes with CKD as activators, the spectrum shifted to a lower wave number at all peaks especially around 1070-950 cm^{-1} corresponded to Si-O stretching vibration of C-S-H gel (tobermorite). This indicated that the alkalinity of the CKD affected phase transformation of samples made of 60% Fly Ash + 30% CEM 1 + 10% CKD (Mix 10).

Change of mineral phase compositions and chemical analysis of the products studied by XRD and XRF

The mineralogical and chemical composition of the cementitious products from crushed paste samples was determined using X-ray diffraction (XRD) and X-ray fluorescence (XRF) techniques and results are shown in Figure 9 and Table 7 respectively.

Mineral phase changes induced by adding CKD can be examined by comparing control mixes (70% fly ash + 30% CEM1) to the optimised mix proportion (60% fly ash + 30% CEM1 + 10%

CKD), i.e. comparing Figures 9(a) & 9(b) for fly ash 1 and Figures 9(d) & 9(e) for fly ash 2. For fly ash 1 pastes, there was no presence of larnite (Ca_2SiO_4) and gibbsite ($Al_2O_3.3H_2O$) in the control paste but they existed in the optimum paste to a higher degree of crystallinity. These minerals have a significance role in relation to strength contribution. For fly ash 2 pastes, there was no presence of larnite (Ca_2SiO_4) in the control paste but it existed in the optimum paste and all the vaterite crystalline changed to calcite, which is more chemically stable. Here, the degree of crystallinity seems to be higher in comparison to the control sample. Comparison of the same samples shows higher intensity for different minerals for samples made with fly ash 1, which confirms more potential of reactivity in fly ash 2. The effectiveness of activation with gypsum can be assessed by comparing control mixes to mixes with 60% fly ash + 30% CEM1 + 10% gypsum, i.e. comparing Figures 9(a) & 9(c) for fly ash 1 and Figures 9(d) & 9(f) for fly ash 2. No new crystalline formed in mixes activated with gypsum relative to the corresponding control mixes. The intensity of identified crystalline major phases increased significantly, which shows more binding water and less strength for the product.

The proportion of reacted fly ash can be found by comparing the proportion of calcium content observed in the paste samples (Table 7) to the total proportion of calcium content in the original mixes. The initial proportion of calcium content in the mixes can be calculated by multiplying the content of individual raw materials (Table 1) by the proportion of the raw materials in a given mix (Table 3) and then calculating the total. The percentage of reacted fly ash was calculated for selected mixes and is presented on the bottom of Table 7. It should be mentioned that the reacted fly ash in different formulation gives rise to the calcium silicate hydrate and alkali calcium silicate hydrate gels in different cases. It is obvious that the percentage of reacted fly ash increases due to adding CKD as activator while adding gypsum for sulphate activation does not increase the reactivity. Due to the chemical composition of applied paste mixes, the CaO content in composites pastes with optimum proportion have increased 33% and 36% compared to control mixes for pastes made from fly ash 1 and fly ash 2, respectively. Comparing the reacted fly ash in both control mixes shows that fly ash 2 has shown 3.6% more reactivity than fly ash 1. Replacing 10% (relative to the total binder) of fly ash with CKD caused increases in the reacted fly ash of 7.71% for fly ash 1 and 7.5% for fly ash 2. However, replacing 10% (relative to the total binder) of fly ash with gypsum caused decreases in the reacted fly ash

relative to the control mix, particularly for fly ash 2. In Table 7, adding gypsum as activator to the mixes made with fly ash 2 increased the amount of silicon, which is likely to be caused by increased dissolution of the fly ash without gel formation. This leads to a weaker gel formation and goes some way to explaining why lower compressive strengths were observed for samples activated with gypsum. The CaO content in composites pastes activated with 10% gypsum was 15% greater than the control mix for fly ash 1 but 18% less than the control mix for fly ash 2. However, when compared to the optimum mixes activated with CKD, the CaO content of the pastes activated with gypsum were 13% and 40% lower, which demonstrates that CKD is more effective in activating fly ash.

Conclusions

Within the current investigation, the following conclusions can be reached:

1. A high volume fly ash paste with a fly ash content of up to 60% of the binder can be designed to achieve appreciable early age compressive strength and a 28 day compressive strength approaching that expected of a binder for a structural grade of concrete.
2. Use of CKD as an activator led to reductions in initial setting times of up to 32% relative to the control pastes.
3. Increases in 2 day strength of 45% and 184% (relative to the respective control paste) were observed for the two fly ashes tested here and corresponding increases in 28 day strength were 15% and 61% when CKD was used as an activator.
4. Use of gypsum as an activator for fly ash is not effective at 2 days but can contribute more effectively at 28 days and beyond. Literature suggests that gypsum is more effective in activating fly ash when used with elevated curing temperatures.
5. No presence of larnite (Ca_2SiO_4) and gibbsite ($Al_2O_3.3H_2O$) has been observed in the control mixes while these existed in the optimum mix and all the vaterite crystalline has changed to calcite, which is more stable. These minerals led to a stronger microstructure in optimum pastes.
6. 60% Fly Ash + 30% CEM 1 + 10% CKD can be considered in future work as an initial optimum binder proportion in HVFA concretes.

7. High volume fly ash paste activated with CKD can be classified as a high alkali cements according to BRE standard. Future work is suggested to assess the likelihood of alkali-aggregate reaction when these paste proportions are used in concrete.

Acknowledgement

This work was supported by the Engineering and Physical Sciences Research Council (EPSRC) under Grant [EP/J016055/1]. The authors gratefully acknowledge the Engineering and Physical Sciences Research Council for funding.

References

[1] R.I., Malek, Z.H., Khalil, S.S.,Imbaby, D.M., Roy, The contribution of class-F fly ash to the strength of cementitious mixtures, Cement and Concrete Research, Vol. 35, (2005), pp. 1152-1154

[2] L.H., Jiang, V.M., Malhotra, Reduction in water demand of non-air-entrained concrete incorporating large volume of fly ash, Cem. Concr. Res., Vol. 30, (2000), pp. 1785-1789

[3] C.D. Atis, High-volume fly ash concrete with high strength and low drying shrinkage, Journal of Material in civil Engineering (ASCE), 15(2), (2003), pp.153-156

[4] N., Bouzoubaâ, M.H., Zhang, V.M., Malhotra, Mechanical properties and durability of concrete made with high-volume fly ash blended cement using a coarse fly ash, Cem. Concr. Res., Vol. 31, (2001), pp. 1393-1402

[5] N., Bouzoubaâ, A., Bilodeau, V., Sivasundaram, and A.K., Chakraborty, Mechanical Properties and Durability Characteristics of High-Volume Fly Ash Concrete Made with Ordinary Portland Cement and Blended Portland Fly Ash Cement, ACI Special Publication, Vol. 242, (2007), pp. 303-320

[6] C.Y., Lee, H.K., Lee, K.M., Lee, Strength and micro structural characteristics of chemically activated fly ash – cement systems, Cem. Concr. Res., Vol. 33, (2003), pp. 425-431

[7] C. Shi, Early microstructure development of activated lime-fly ash pastes, Cem. Concr. Res., Vol. 26(9), (1996), pp. 1351-1359

[8] J., Qian, C., Shi, Z., Wang, Activation of blended cements containing fly ash, Cem. Concr. Res., Vol. 31, (2001), pp. 1121-1127

[9] D.P., Bentz, Powder Additions to Mitigate Retardation in High-Volume Fly Ash Mixtures, ACI Materials Journal, Vol. 107, No. 5, (2010), pp. 508-514

[10] S.W.M. Supit, F.U.A. Shaikh, Effect of Nano-$CaCO_3$ on Compressive Strength Development of High Volume Fly Ash Mortars and Concretes, Journal of Advanced Concrete Technology, Vol.12, (2014), pp. 178-186

[11] M.S., Konsta-Gdoutos, S.P., Shah, Hydration and properties of novel blended cements based on cement kiln dust and blast furnace slag, Cem. Concr. Res., Vol. 33, (2003), pp. 1269-1276

[12] Alkali–silica reaction in concrete detailed guidance for new construction, BRE Digest 330, (2004)

[13] M.S.Y., Bhatty, Alternative Uses of Cement Kiln Dust, RP 327, Portland cement Association, Skokie, Illinois, U.S.A. (1955)

[14] M.S.Y., Bhatty, Use of Cement Kiln Dust in Blended Cements, World Cement Technology, London, U.K., Vol. 15, No. 4, (1984), PP. 126-128

[15] M.S.Y., Bhatty, Use of Cement Kiln Dust in Blended Cements: Alkali- Aggregate Reaction Expansion, World Cement Technology, London, U.K., Vol. 16, No. 10, (1985), PP. 386-392

[16] M., Maslehuddin, O.S.B., Al-Amoudi, M., Kalimur Rahman, M., Shameem, Use of cement kiln dust in blended cement concrete, Proceedings of the Institution of Civil Engineers and Construction Materials, Vol. 63, (2009), pp. 149-156

[17] M., Maslehuddin, O.S.B., Al-Amoudi, M., Shameem, M.K., Rahman, M., Ibrahim, Use of cement kiln dust in cement products-research review and preliminary investigations, Construction and Building Materials, Vol. 22, (2008), pp. 2369-2375

[18] K. Wang, M. S. Konsta-Gdoutos, and S. P. Shah, Hydration, Rheology, and Strength of CKD-Slag-OPC Binders, ACI Material Journal, Vol. 99, No. 2, (2002), pp. 173-179

[19] M.S. Konsta-Gdoutos, S.P. Shah, Hydration and properties of novel blended cements based on cement klin dust and blast furnace slag, Cem. Concr. Res., Vol. 33, (2003), pp. 1269-1276

[20] K. Wang, S. P. Shah, A. Mishulovich, Effects of curing temperature and NaOH addition on hydration and strength development of clinker-free CKD-fly ash binders, Cem. Concr. Res., Vol. 34, (2004), pp. 299-309

[21] K. Wang, A. Mishulovich, S.P. Shah, Activations and Properties of Cementitious Materials Made with Cement-Klin Dust and Class-F Fly ash, Journal of Material in civil Engineering (ASCE), 19(1), (2007), pp.112-119

[22] C.S., Poon, S.C., Kou, L., Lam, Z.S., Lin, Activation of fly ash/cement systems using calcium sulfate anhydrite (CaSO4), Cem. Concr. Res., Vol. 31, (2001), pp. 873-881

[23] A.A. Ramezanianpour, F. Alapour, Compressive strength of fly ash geopolymer paste designed by Taguchi method, in 3rd International Conference on Sustainable Construction Materials and Technologies, (2013), Kyoto, Japan

497 Table 1: Relative oxide content and loss on ignition (LOI) of the materials

498

Oxides	Percentage				
	Fly ash 1	**Fly ash 2**	**CEM 1**	**CKD**	**GYPSUM**
SiO_2	52.15	51.16	19.63	15.46	3.92
TiO_2	0.87	1.01	0.26	0.23	0.05
Al_2O_3	19.61	24.34	4.71	3.80	1.10
Fe_2O_3	7.10	10.17	3.25	2.55	0.48
MnO	0.07	0.05	0.09	0.08	0.01
MgO	2.00	1.46	1.17	0.97	0.68
CaO	4.40	2.79	64.09	54.18	42.61
Na_2O	1.06	1.28	0.27	0.56	0.18
K_2O	1.93	2.57	0.73	4.90	0.17
P_2O_5	0.45	0.35	0.20	0.15	0.03
SO_3	0.54	0.26	2.94	3.84	43.70
LOI	9.48	4.35	3.22	13.25	7.59
Total	99.67	99.79	100.55	99.96	100.51

499

500 Table 2: Physical properties of materials

501

Material	**Density (g/cm^3)**	**Fineness (cm^2/g)**
CEM 1	3.205	3493
Fly ash 1	1.950	4699
Fly ash 2	2.096	4506
CKD	2.734	2490
Gypsum	2.300	3470

502

503 Table 3: Different proportions used to optimize the binder constituents

504

Mix No.	Fly Ash (%)	CEM 1 (%)	CKD (%)	Gypsum (%)
1	70	30	0	0
2	70	25	5	0
3	70	25	0	5
4	70	20	10	0
5	65	30	0	5
6	65	25	10	0
7	65	25	5	5
8	65	20	10	5
9	65	20	5	10
10	60	30	10	0
11	60	30	0	10
12	60	25	5	10
13	60	20	10	10

505

506

507

508

509

510

511

512

513

514

515

516

517 Table 4a: Setting time properties of selected binders made using fly ash 1

518

Binder Type / Setting Property	Control Binder Without Plasticiser	Control Binder With Plasticiser	Optimized Binder 1 Without Plasticiser	Optimized Binder 1 With Plasticiser
Consistence (%)	**35**	**29**	**37**	**31**
Initial Setting Time (min)	**155**	**95**	**105**	**90**
Final Setting Time (min)	**215**	**210**	**155**	**140**

519

520

521 Table 4b: Setting time properties of selected binders made using fly ash 2

522

Binder Type / Setting Property	Control Binder Without Plasticiser	Control Binder With Plasticiser	Optimized Binder 2 Without Plasticiser	Optimized Binder 2 With Plasticiser
Consistence (%)	**29**	**23**	**30**	**27**
Initial Setting Time (min)	**185**	**105**	**125**	**100**
Final Setting Time (min)	**245**	**230**	**185**	**165**

523

524 Table 5a: S/N ratio of the early age compressive strength tests for fly ash 1 pastes

Mix No.	Fly Ash (%)	CEM 1 (%)	CKD (%)	Gypsum (%)	Y1	Y2	Y3	S/N
1	70	30	0	0	7.68	7.47	7.89	17.70
2	70	25	5	0	8.33	6.38	10.28	17.92
3	70	25	0	5	4.08	3.39	4.77	11.96
4	70	20	10	0	5.08	4.95	5.21	14.11
5	65	30	0	5	4.25	4.25	4.25	12.57
6	65	25	10	0	9.12	5.29	12.95	17.47
7	65	25	5	5	6.06	4.5	8.00	15.05
8	65	20	10	5	4.55	3.37	5.73	12.55
9	65	20	5	10	5.38	5.27	5.49	14.61
10	60	30	10	0	11.11	7.68	14.54	**20.03**
11	60	30	0	10	5.22	4.25	6.19	14.05
12	60	25	5	10	5.41	5.24	5.58	14.66
13	60	20	10	10	3.27	3.20	3.34	10.29

525

526 Table 5b: S/N ratio of the early age compressive strength tests for fly ash 2 pastes

Mix No.	Fly Ash (%)	CEM 1 (%)	CKD (%)	Gypsum (%)	Y1	Y2	Y3	S/N
1	70	30	0	0	5.76	3.97	7.55	14.31
2	70	25	5	0	12.89	11.96	13.82	22.16
3	70	25	0	5	2.90	2.60	3.2	9.15
4	70	20	10	0	8.30	5.10	11.5	16.95
5	65	30	0	5	4.97	4.55	5.39	13.86
6	65	25	10	0	12.95	9.35	16.55	21.54
7	65	25	5	5	6.32	4.73	7.91	15.44
8	65	20	10	5	6.88	4.15	9.61	15.23
9	65	20	5	10	3.13	2.76	3.5	9.79
10	60	30	10	0	16.36	19.18	13.54	**24.01**
11	60	30	0	10	4.56	4.33	4.79	13.16
12	60	25	5	10	4.18	3.23	5.13	11.96
13	60	20	10	10	3.41	2.90	3.92	10.46

527 Table 6a: S/N ratio response table for fly ash 1 pastes

528

Factor/Level	J=1	J=2	J=3	J=4	M_4	J=5	M_5
FA/1(60%)	14.05	10.29	14.66	20.03	14.76		
FA/2(65%)	12.55	14.61	15.05	12.57	13.70	17.47	14.45
FA/3(70%)	14.11	17.92	11.96	17.7	**15.42**		
CEM1/1(20%)	10.29	12.55	14.61	14.11	12.89		
CEM1/2(25%)	14.66	17.47	15.05	11.96	14.79	17.92	15.41
CEM1/3(30%)	14.05	20.03	12.57	17.7	**16.09**		
CKD/1(0%)	14.05	12.57	11.96	17.7	14.07		
CKD/2(5%)	14.66	14.61	15.05	17.92	**15.56**		
CKD/3(10%)	10.29	12.55	17.47	14.11	13.61	20.03	14.89
GYPS/1(0%)	17.47	14.11	17.92	17.7	**16.8**	20.03	**17.45**
GYPS/2(5%)	12.55	15.05	12.57	11.96	13.03		
GYPS/3(10%)	14.05	10.29	14.66	14.61	13.40		

529

530 Table 6b: S/N ratio response table for fly ash 2 pastes

531

Factor/Level	J=1	J=2	J=3	J=4	M_4	J=5	M_5
FA/1(60%)	13.16	10.45	11.96	24.01	14.9		
FA/2(65%)	15.23	9.79	15.44	13.86	13.58	21.54	15.17
FA/3(70%)	16.95	22.16	9.15	14.31	**15.64**		
CEM1/1(20%)	10.45	15.22	9.79	16.95	13.10		
CEM1/2(25%)	11.96	21.54	15.44	22.16	17.78	9.15	16.05
CEM1/3(30%)	13.16	24.01	13.86	14.31	**16.34**		
CKD/1(0%)	13.16	13.86	9.15	14.31	12.62		
CKD/2(5%)	11.95	9.79	15.44	22.16	14.84		
CKD/3(10%)	10.46	15.23	21.54	16.95	**16.05**	24.01	**17.64**
GYPS/1(0%)	21.53	16.95	22.15	14.31	**18.74**	24.01	**19.79**
GYPS/2(5%)	15.23	15.44	13.86	9.15	13.42		
GYPS/3(10%)	13.16	10.46	11.95	9.78	11.34		

532 Table 7: Relative oxide content, loss on ignition (LOI) and percentage of reacted fly ash in the products

533

Oxides	Percentage					
	Mix1-F1 (70%Fly ash+ 30%CEM1)	**Mix10-F1** (60%Fly ash+ 30%CEM1+ 10%CKD)	**Mix11-F1** (60%Fly ash+ 30%CEM1+ 10%Gypsum)	**Mix1-F2** (70%Fly ash+ 30%CEM1)	**Mix10-F2** (60%Fly ash+ 30%CEM1+ 10%CKD)	**Mix11-F2** (60%Fly ash+ 30%CEM1+ 10%Gypsum)
SiO_2	38.88	35.34	35.36	37.23	34.30	40.996
TiO_2	0.653	0.590	0.583	0.716	0.649	0.767
Al_2O_3	13.92	12.22	12.16	16.42	14.43	17.809
Fe_2O_3	5.07	4.62	4.56	6.76	6.09	7.328
MnO	0.046	0.043	0.043	0.034	0.035	0.039
MgO	1.58	1.49	1.50	1.21	1.19	1.336
CaO	19.83	26.36	22.83	19.59	26.55	16.03
Na_2O	0.74	0.61	0.68	0.80	0.74	0.89
K_2O	1.43	1.28	1.39	1.79	1.78	1.92
P_2O_5	0.311	0.281	0.272	0.247	0.222	0.258
SO_3	1.83	2.17	4.82	1.94	2.64	3.79
LOI	15.44	14.61	15.93	12.85	11.36	8.96
Total	99.63	99.63	100.14	99.58	99.98	100.12
Reacted fly ash	88.9	96.61	87.4	92.5	100	63.70

534

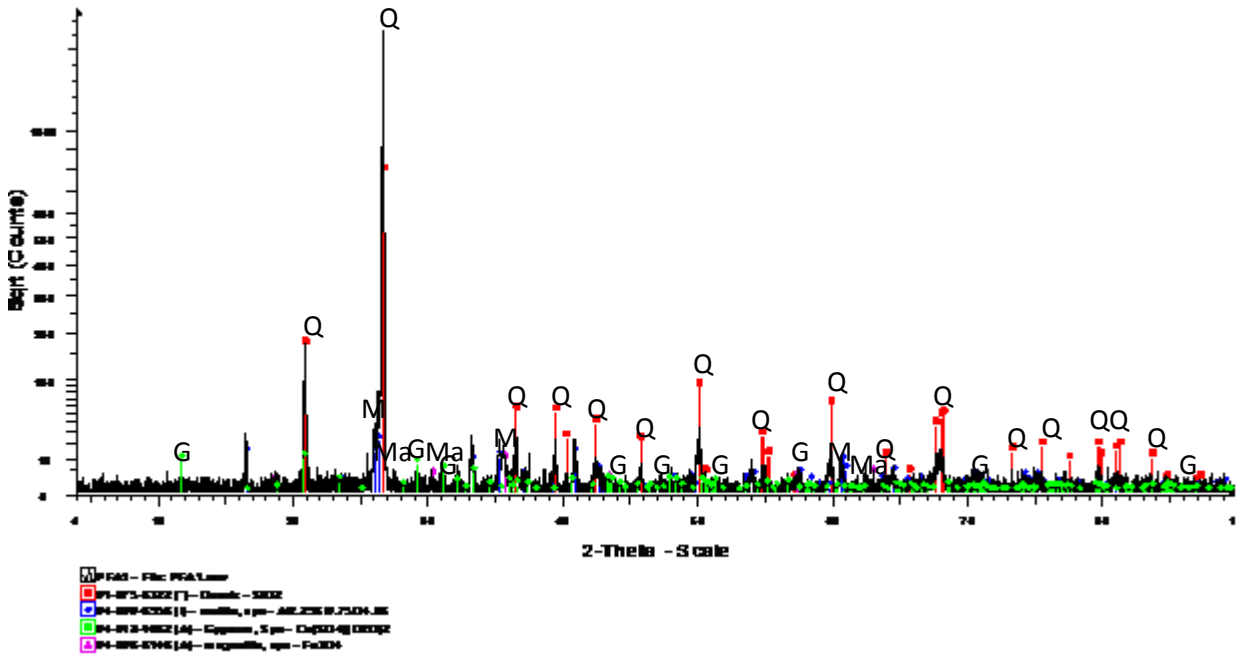

535

536 (a) Fly ash 1

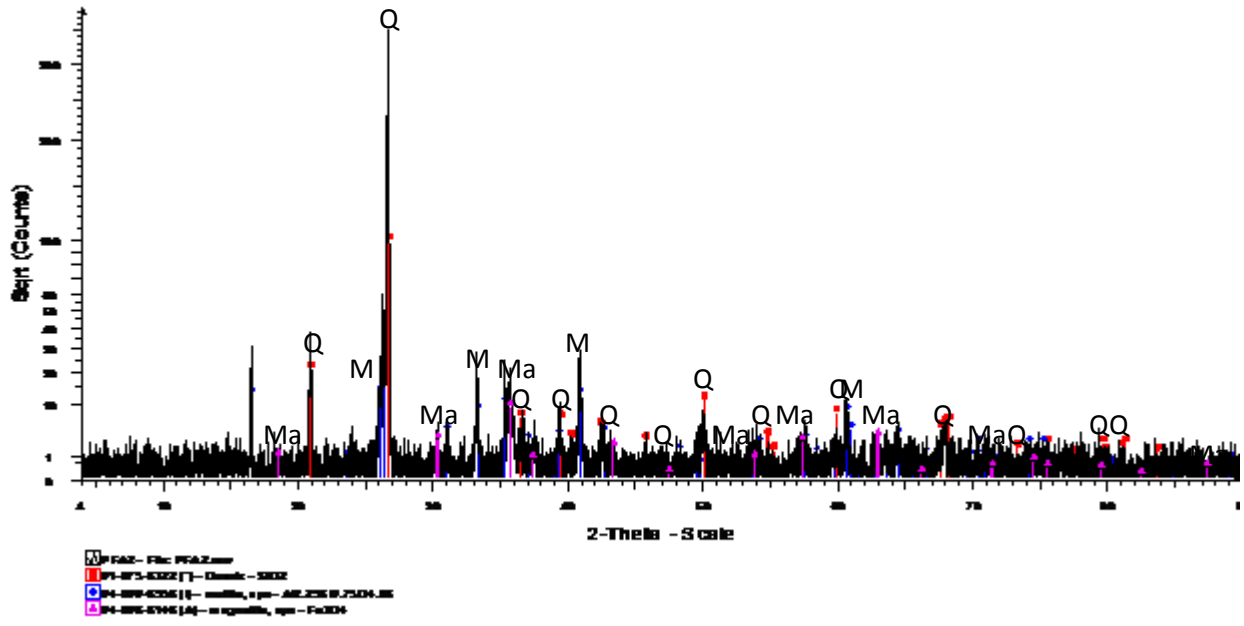

537

538 (b) Fly ash 2

539 Figure 1 (a) and (b) Mineralogical composition of Fly ash 1 and Fly ash 2[G=Gypsum, Ma=Magnetite,

540 M=Mulite, Q=Quartz]

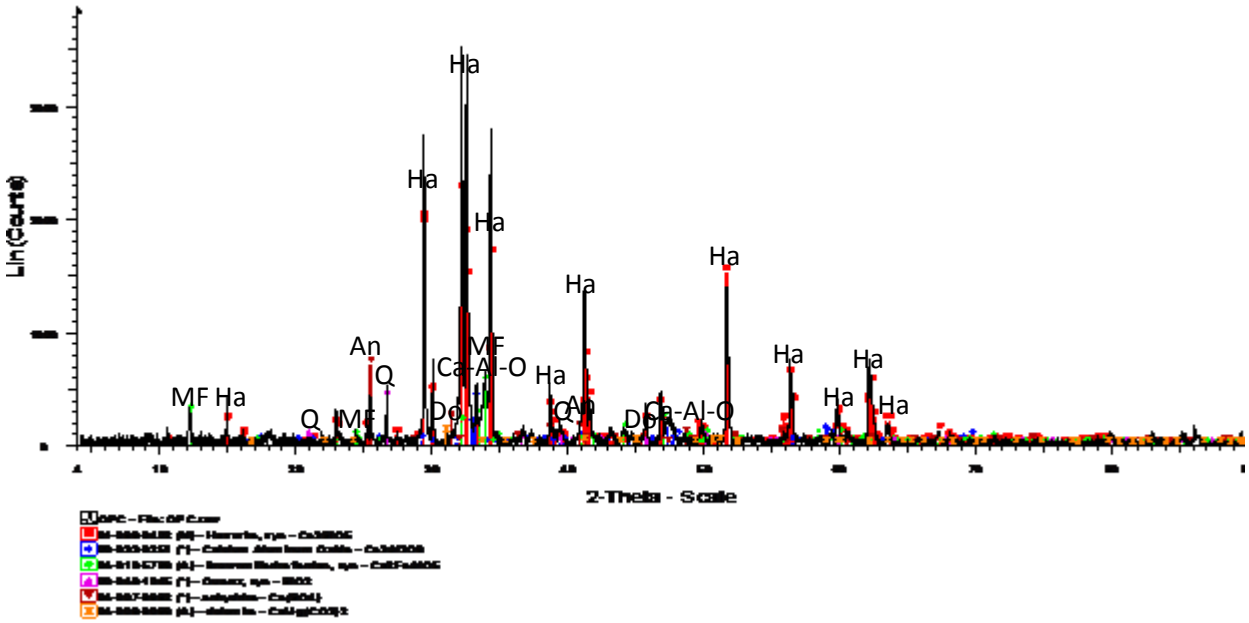

(c) CEM 1

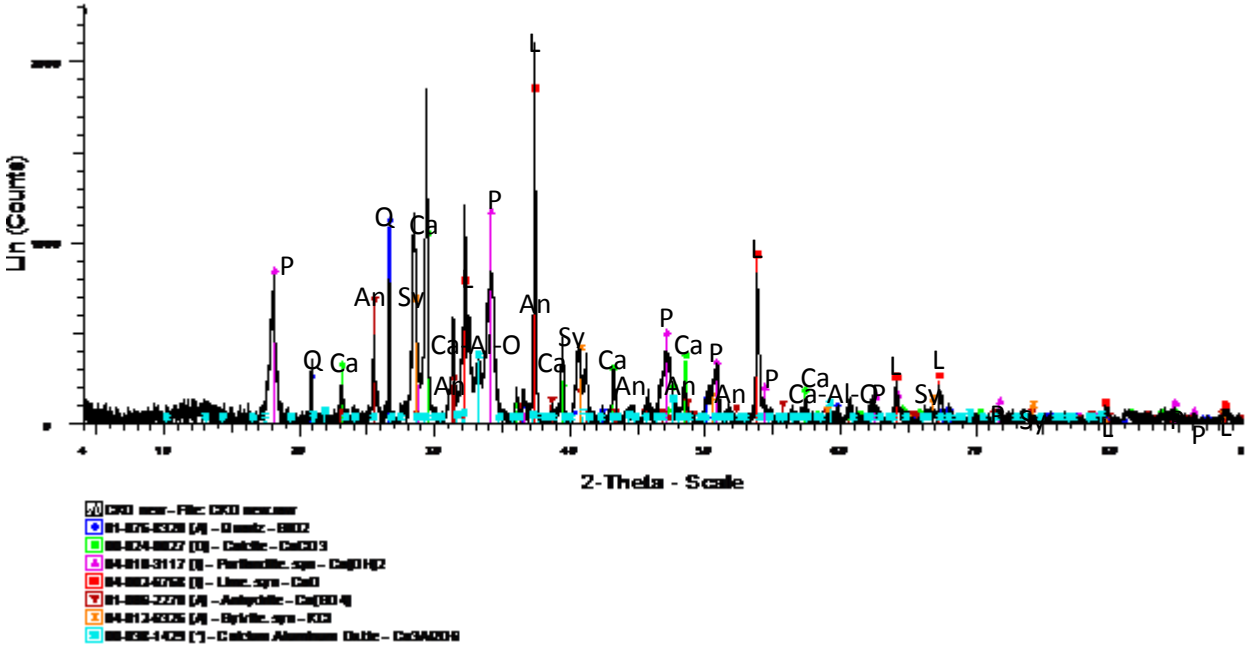

(d) CKD

Figure 1 (c) and (d) Mineralogical composition of CEM 1 and CKD [An=Anhydrite, Ca-Al-O=Calcium Aluminum Oxide, Ca=Calcite, Do=Dolomite, Ha=Hatrurite, L=Lime, MF=Brown Millerite Ferian, P=Portlandite, Q=Quartz, Sy=Sylvite]

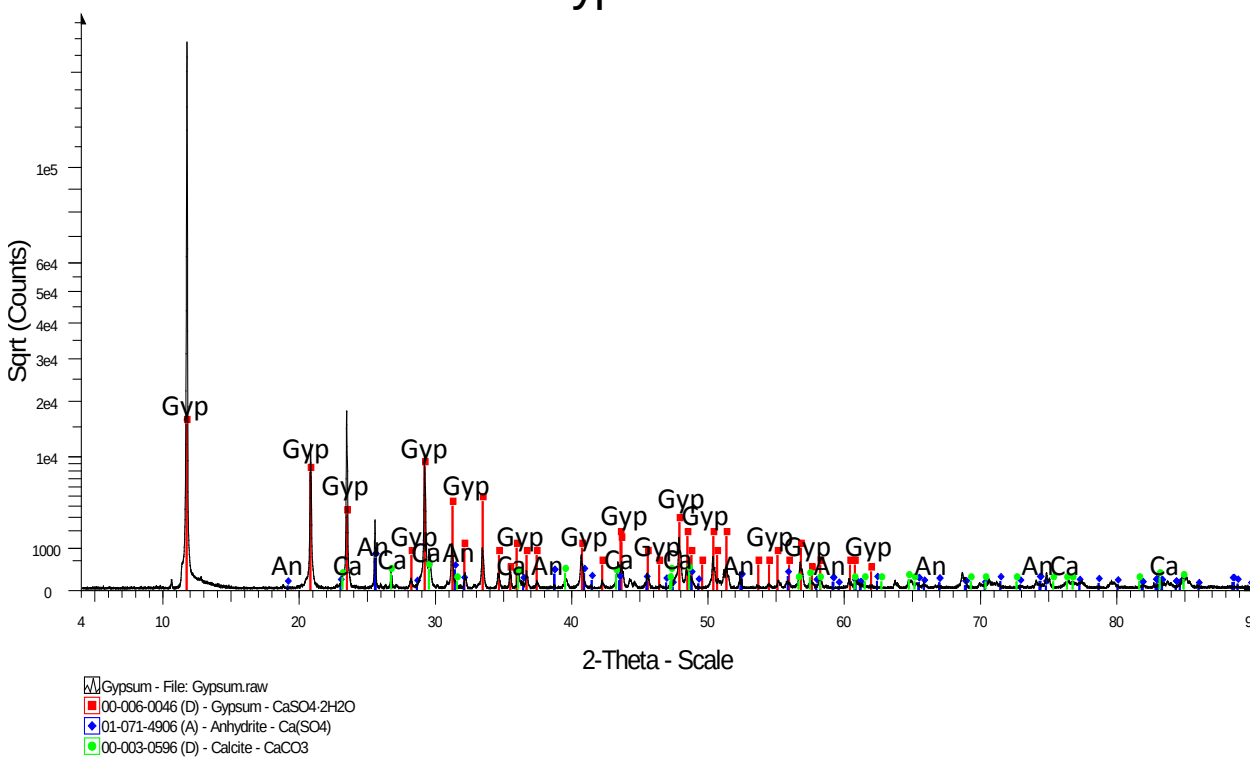

(e) Gypsum

Figure 1 (e) Mineralogical composition of Gypsum [An=Anhydrite, Ca=Calcite, Gyp=Gypsum]

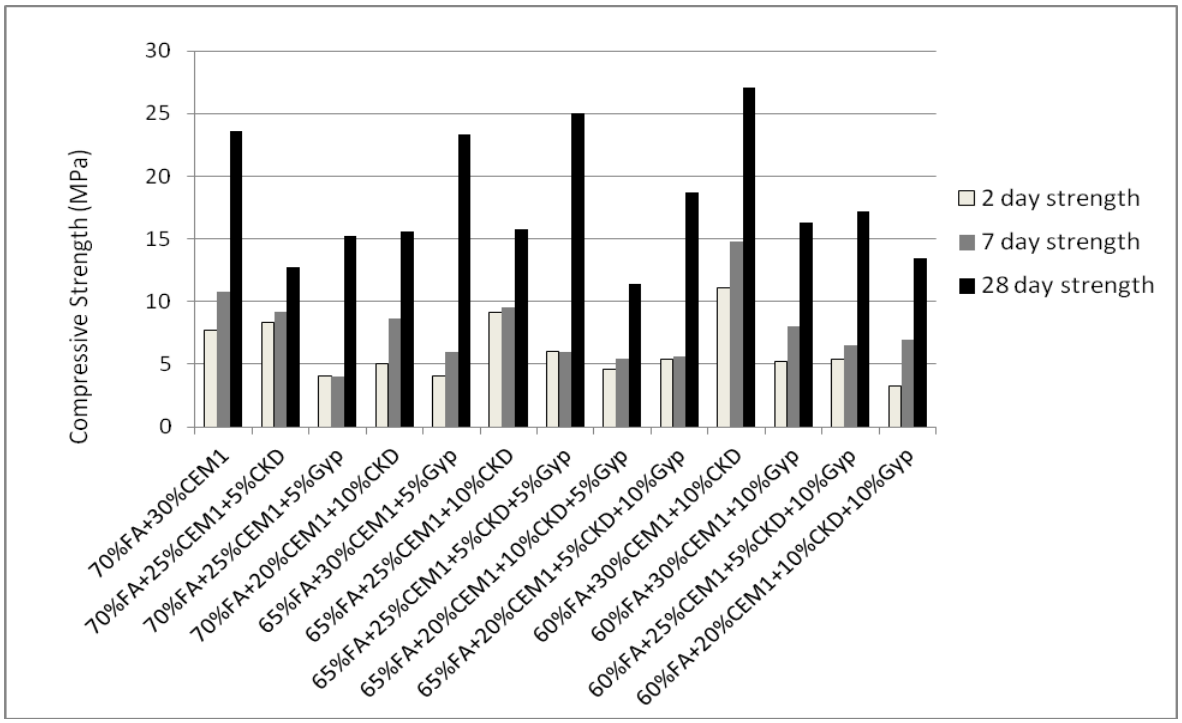

(a)

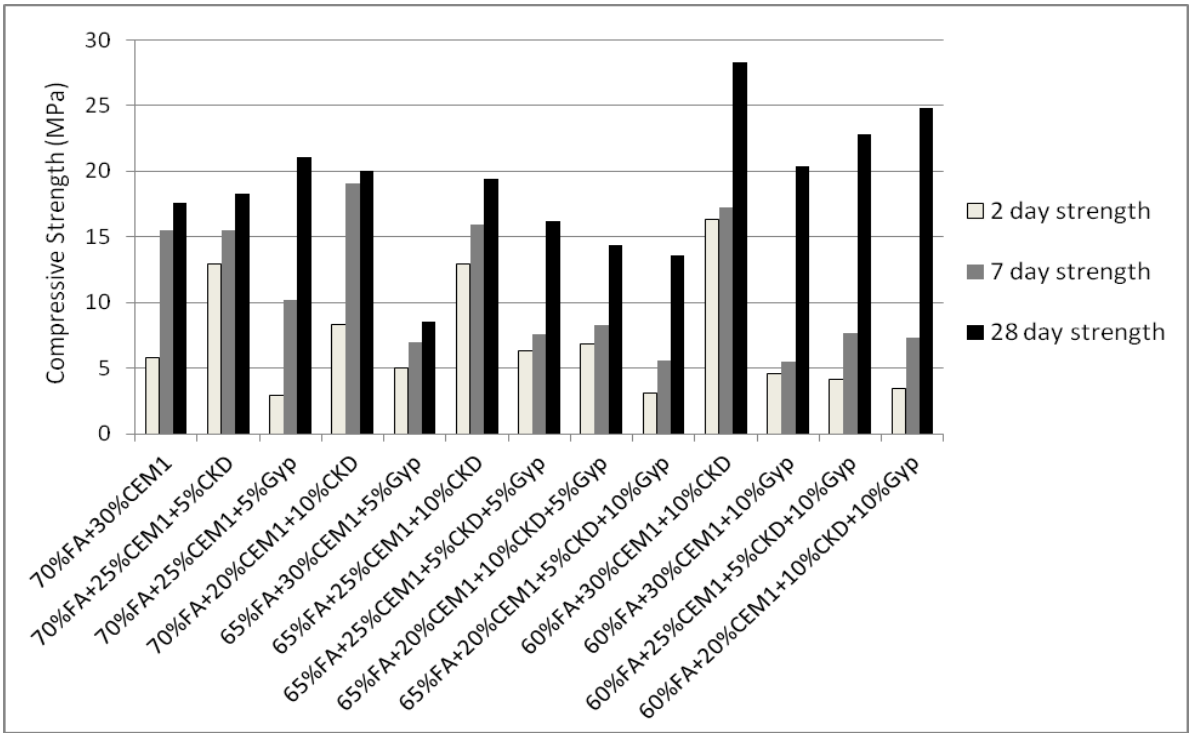

(b)

Figure 2: Compressive strength of HVFA blended pastes at 2, 7 and 28 days for (a) fly ash 1 pastes and (b) fly ash 2 pastes

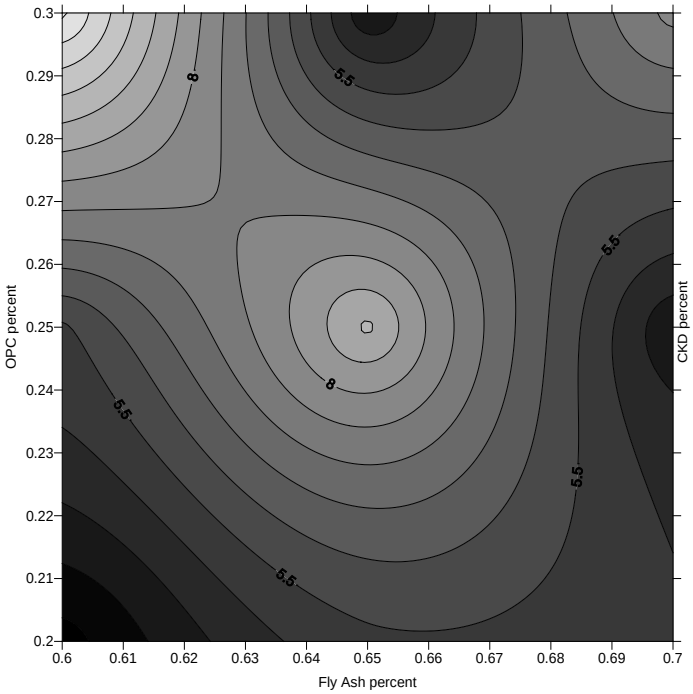

(a) OPC vs. Fly ash

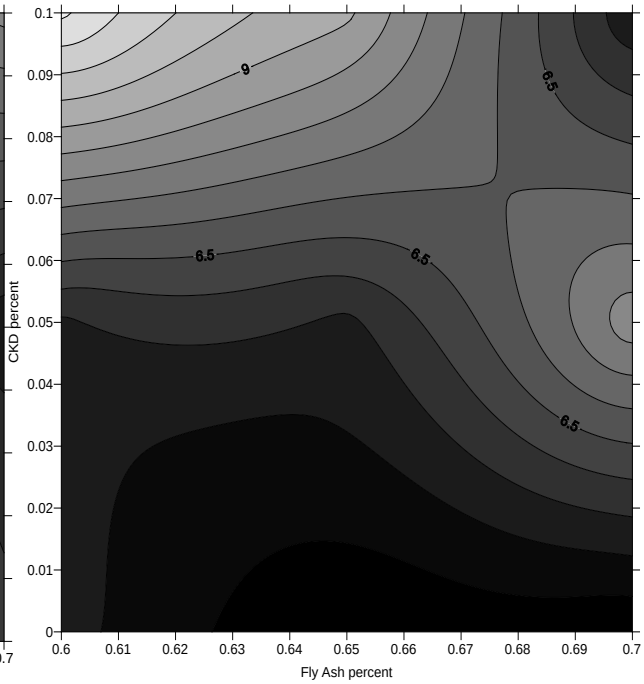

(b) CKD vs. Fly ash

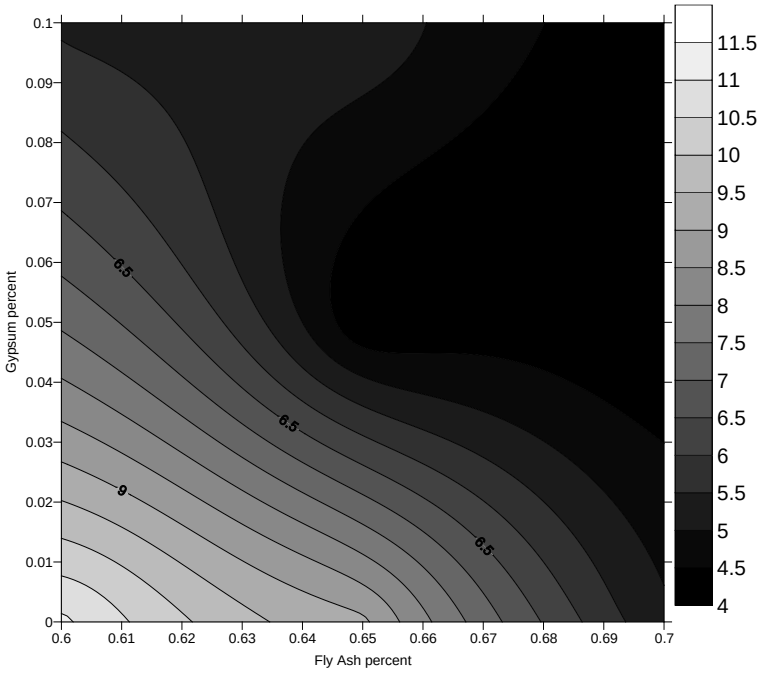

(c) Gypsum vs. Fly ash

Figure 3: Proportion optimisation by Surfer software based on 2 days strength for fly ash 1 pastes

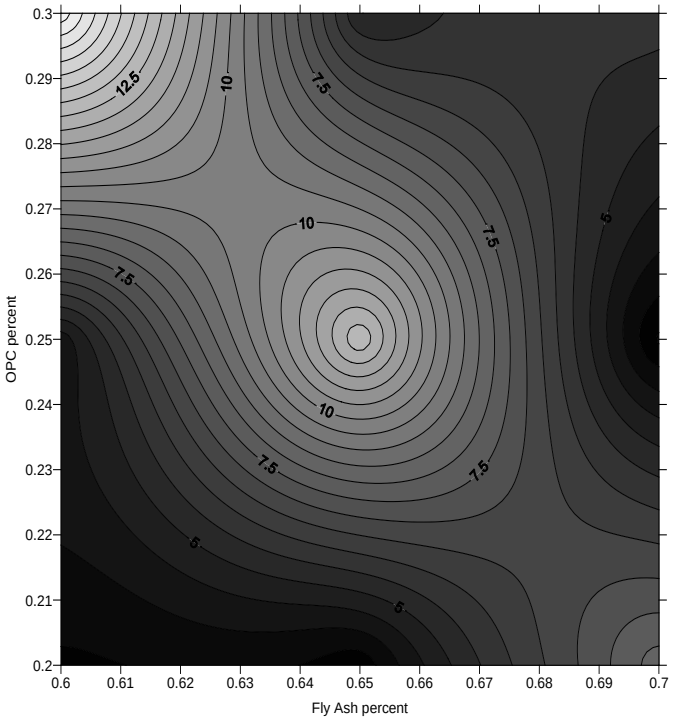

(a) OPC vs. Fly ash

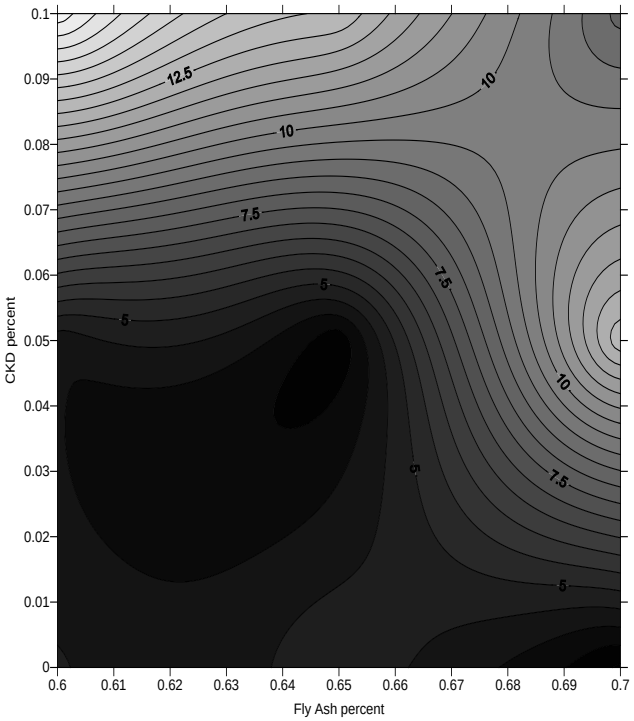

(b) CKD vs. Fly ash

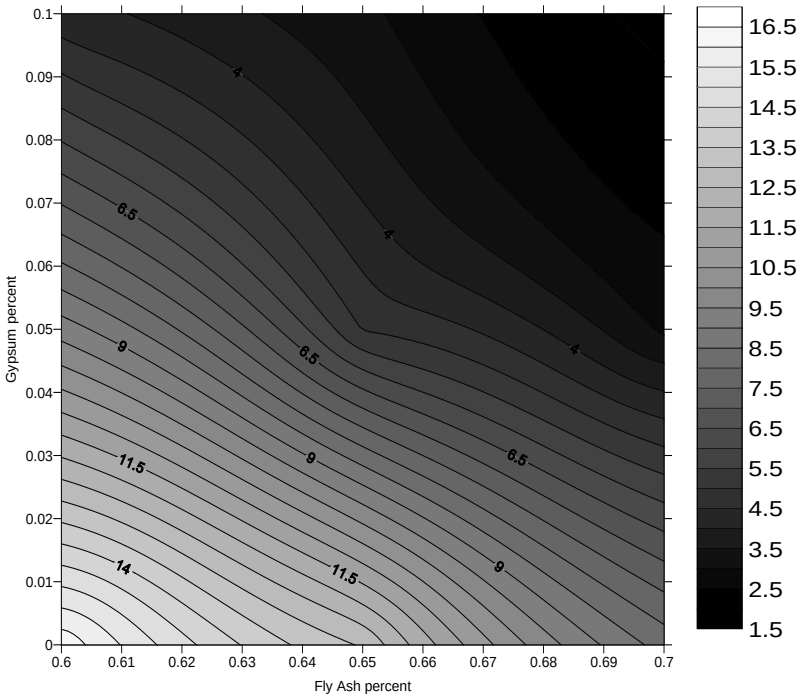

(c) Gypsum vs. Fly ash

Figure 4: Proportion optimisation by Surfer software based on 2 days strength for fly ash 2 pastes

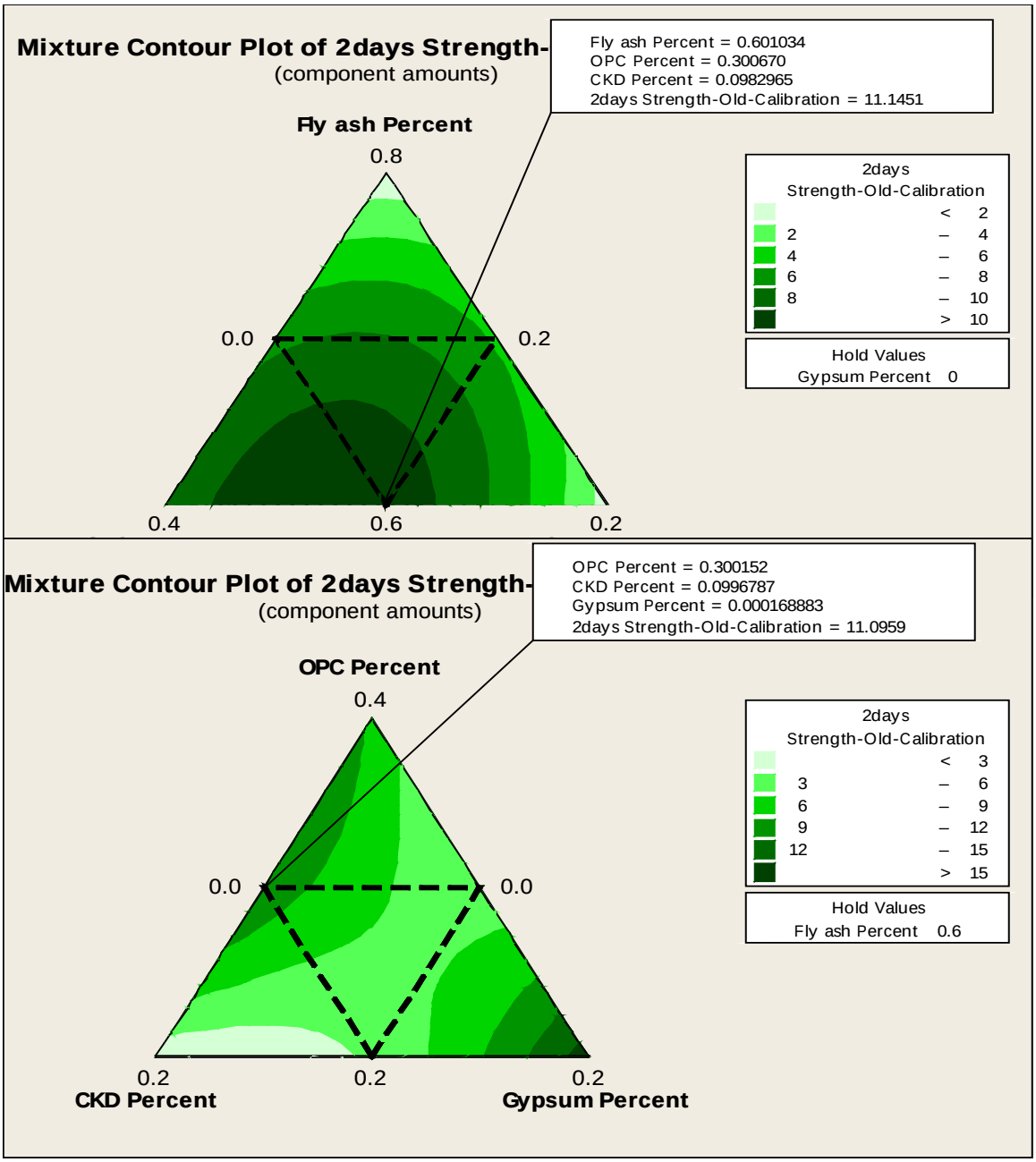

Figure 5: Proportion optimization by Minitab based on 2 days strength for fly ash 1 pastes

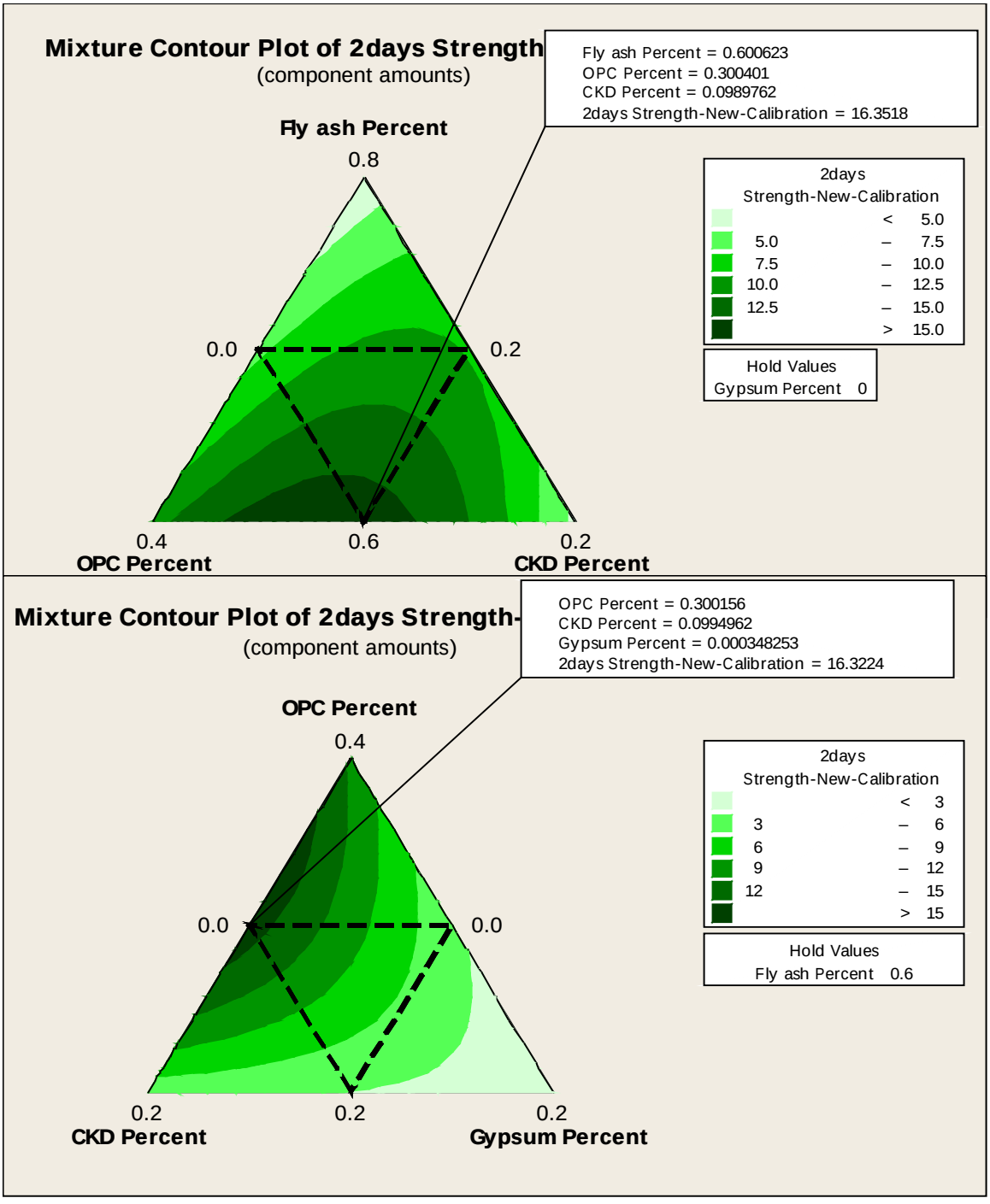

Figure 6: Proportion optimisation by Minitab software based on 2 days strength for fly ash 2 pastes

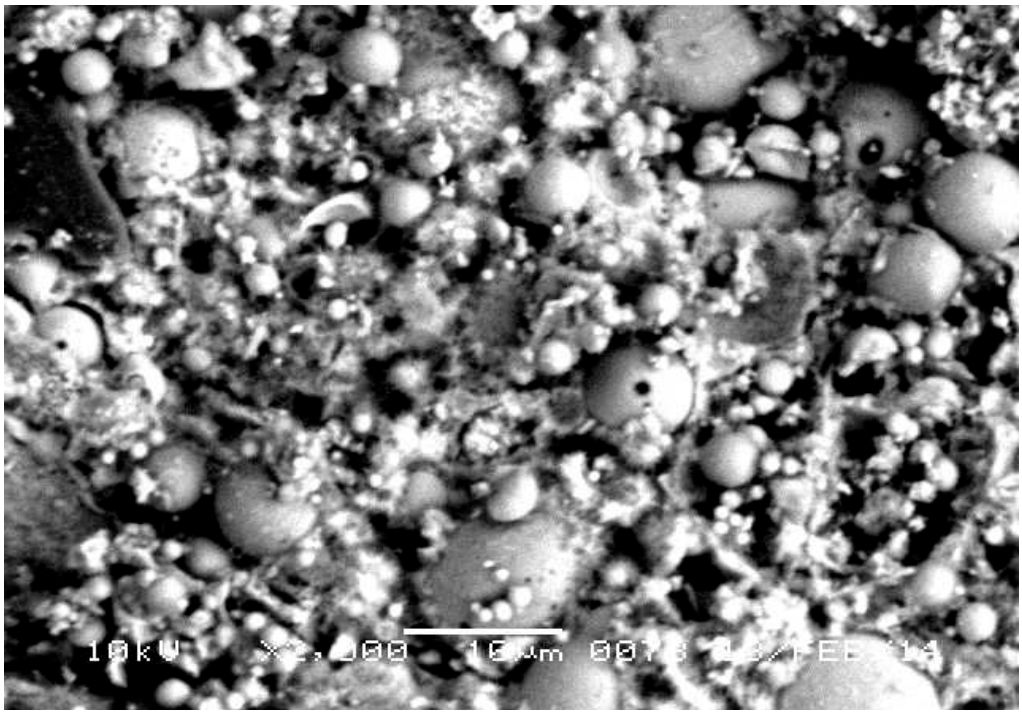

Figure 7(a) Mix 1 for fly ash 1 (70% Fly ash 1+ 30% CEM 1)

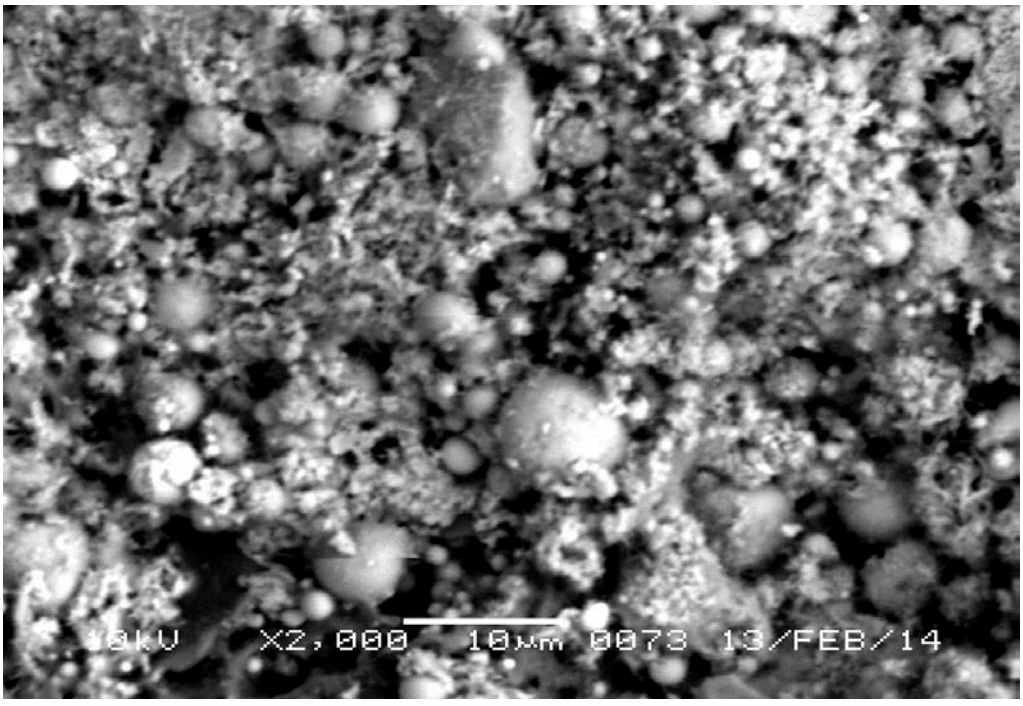

Figure 7(b) Mix 2 for fly ash 1 (70% Fly ash 1+ 25% CEM 1 + 5% CKD)

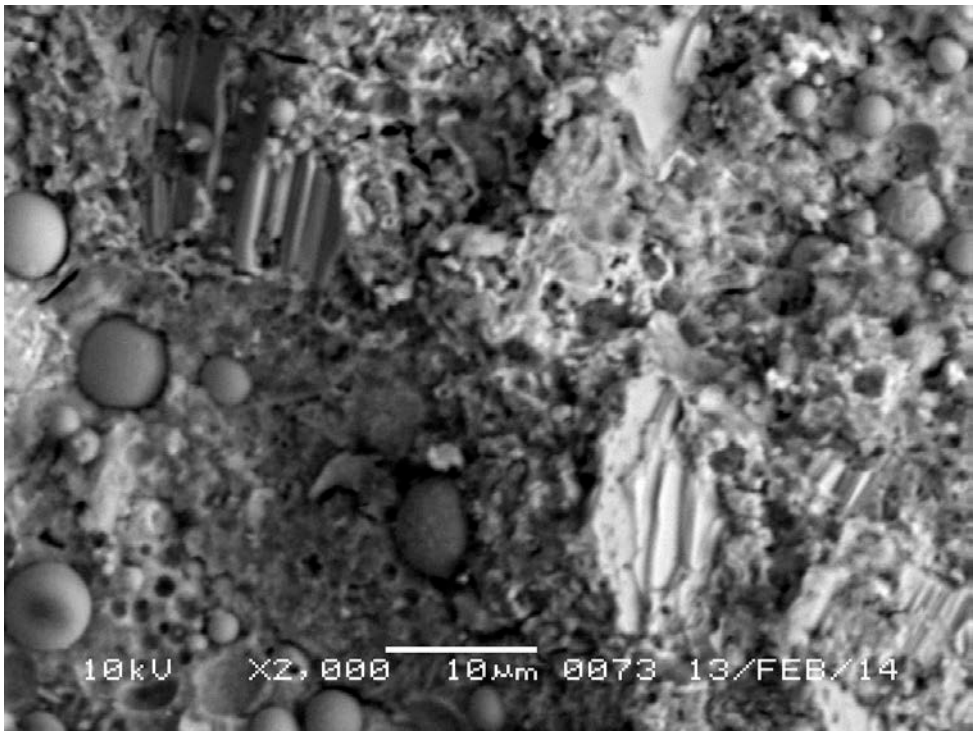

Figure 7(c) Mix 10 for fly ash 1 (60% Fly ash 1+ 30% CEM 1 + 10% CKD)

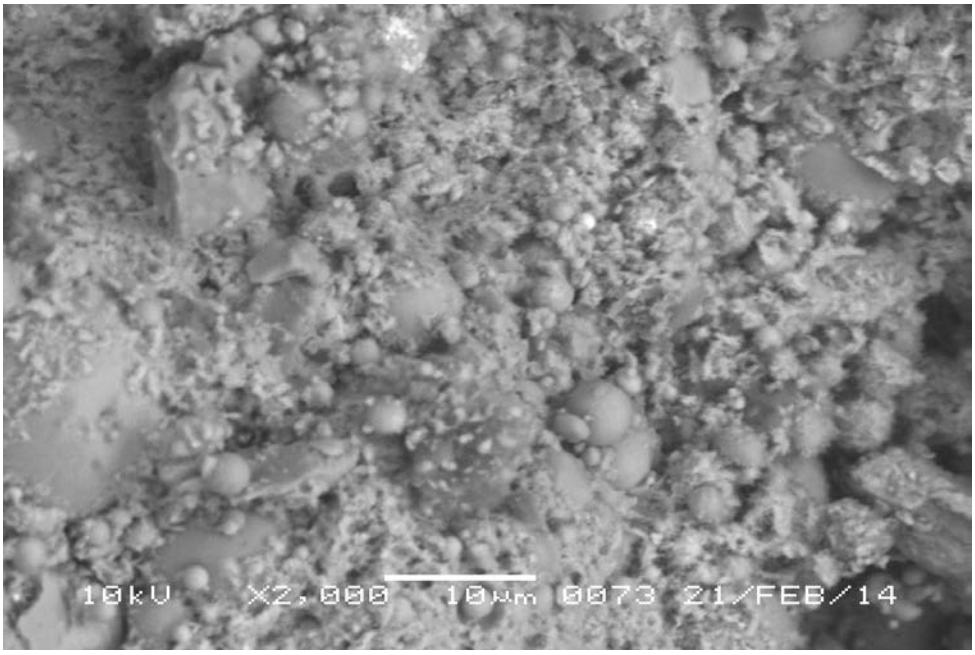

Figure 7(d) Mix 11for fly ash 1 (60% Fly ash 1 + 30% CEM 1+ 10% Gypsum)

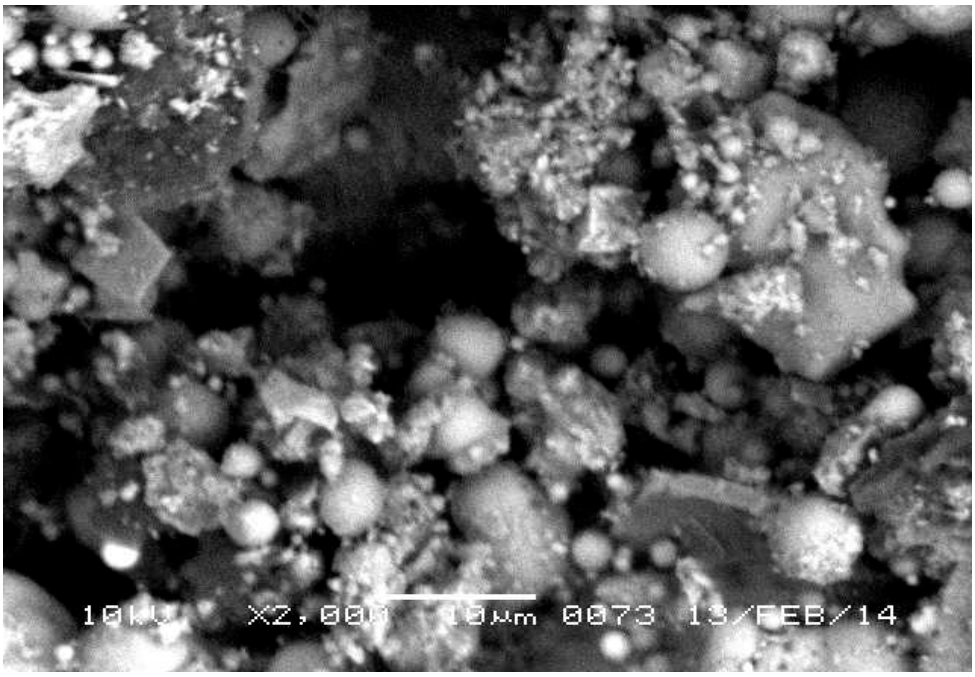

Figure 7(e) Mix 1 for fly ash 2 (70% Fly ash 2 + 30% CEM 1)

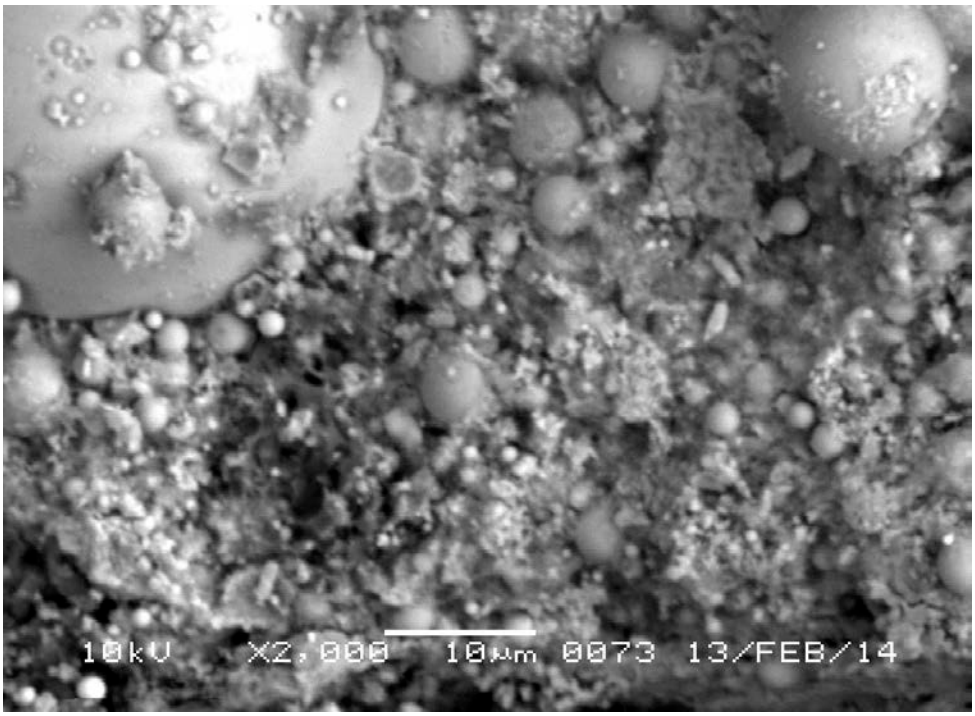

Figure 7(f) Mix 2 for fly ash 2 (70% Fly ash 2 + 25% CEM 1 + 5% CKD)

Figure 7(g) Mix 10 for fly ash 2 (60% Fly ash 2 + 30% CEM 1+ 10%CKD)

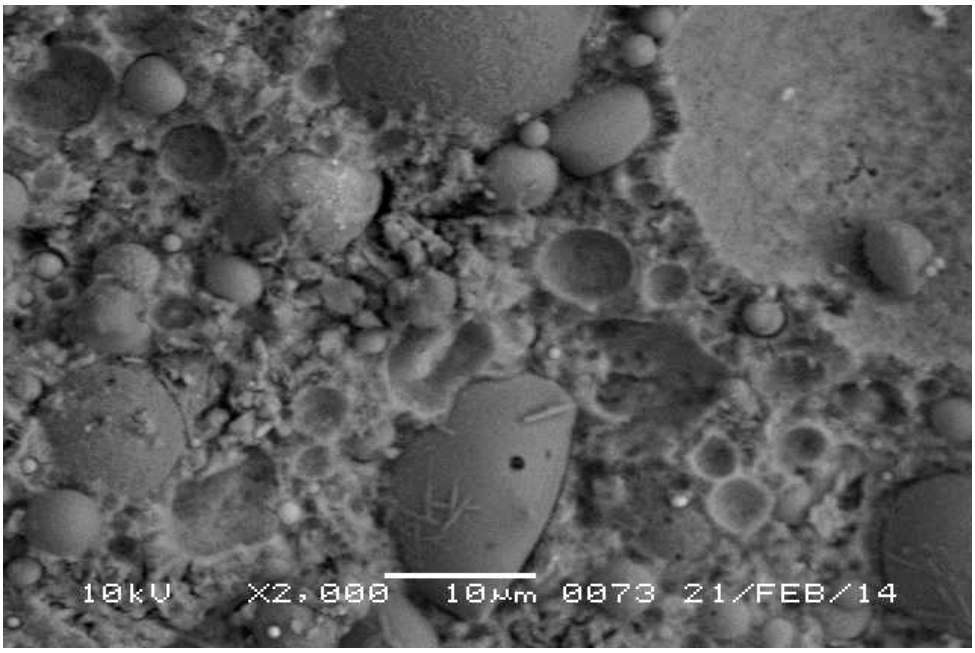

Figure 7(h) Mix 11for fly ash 2 (60% Fly ash 2 + 30% CEM 1 + 10% Gypsum)

Figure 7: SEM images of micro-structure of selected mixes

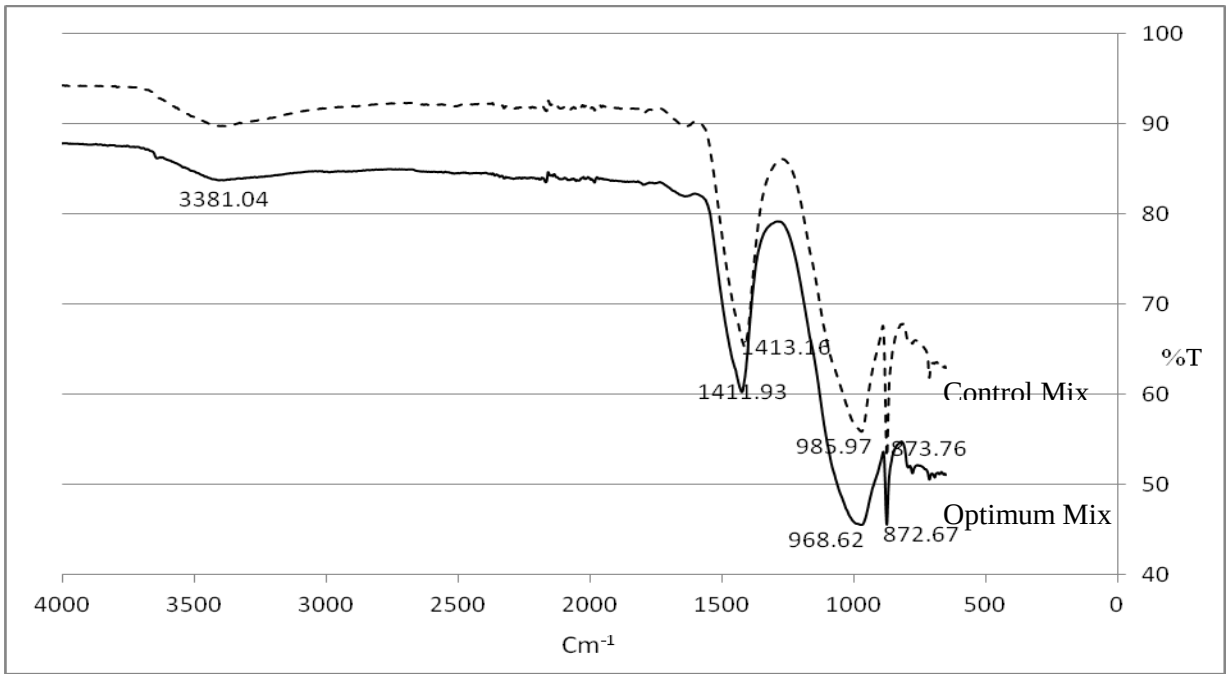

(a) Control mix (70% Fly ash1+ 30% CEM 1) & Optimum Mix (60% Fly ash 1+ 30% CEM 1 + 10%CKD)

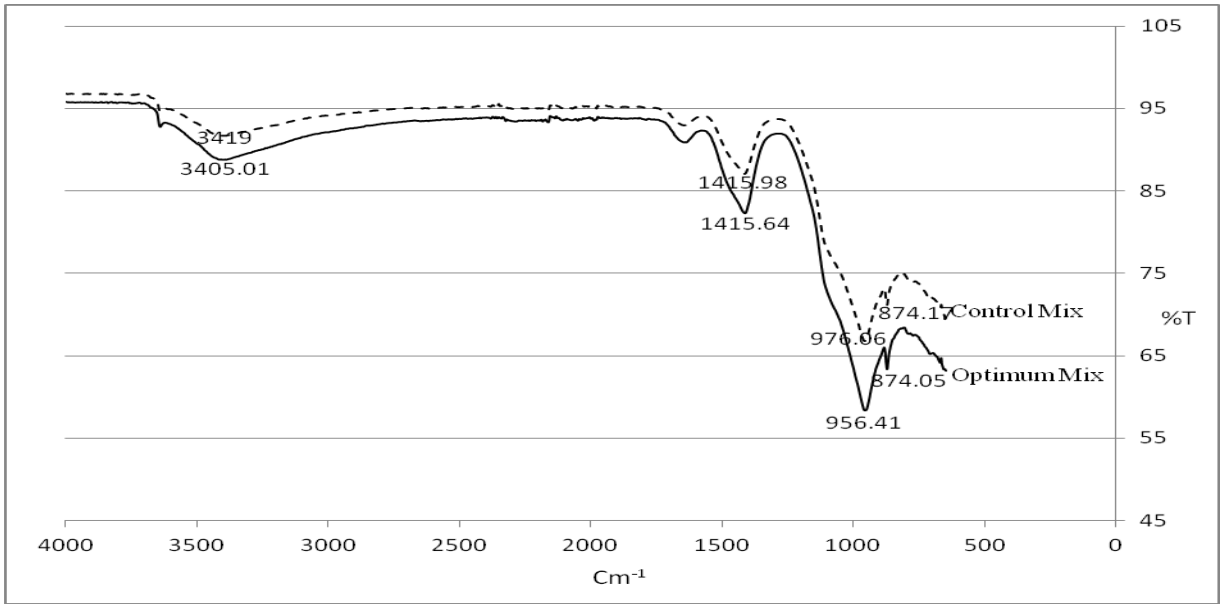

(b) Control mix (70% Fly ash2+ 30% CEM 1) & Optimum Mix (60% Fly ash2+ 30% CEM 1 + 10%CKD)

Figure 8 (a) and (b) FTIR spectra of pozzolanic reaction products resulted from control and optimum mixes of fly ash 1 and 2

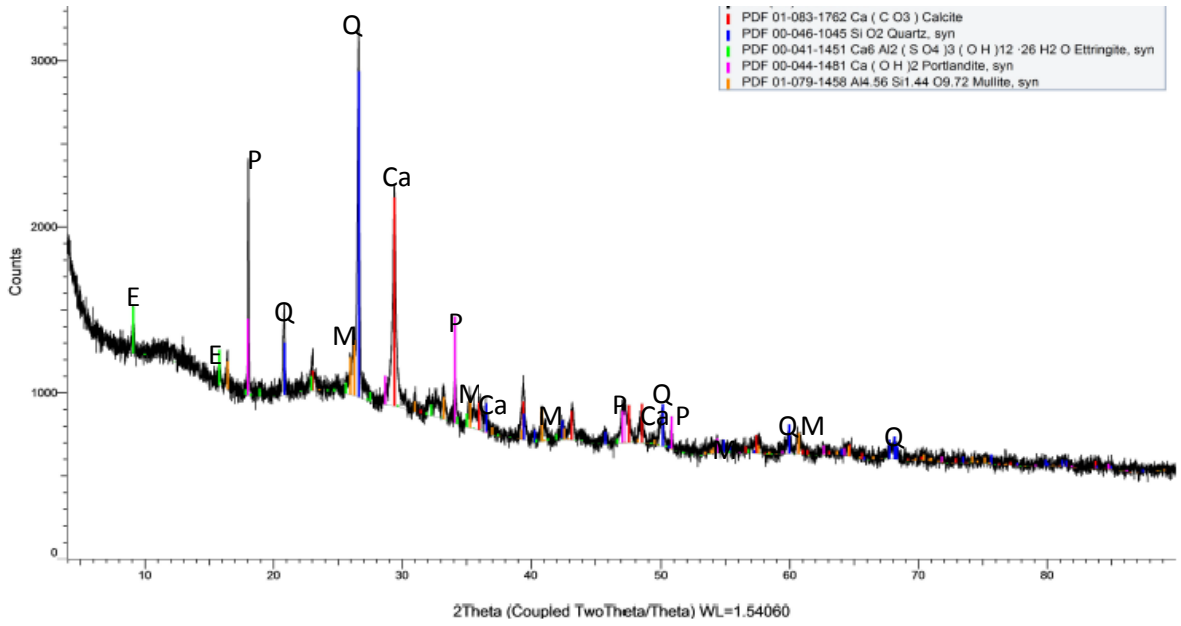

Figure 9(a) Mix 1-F1 (70% Fly ash 1+ 30% CEM 1) [Ca=Calcite, E=Ettringite, M=Mulite, P=Portlandite, Q=Quartz]

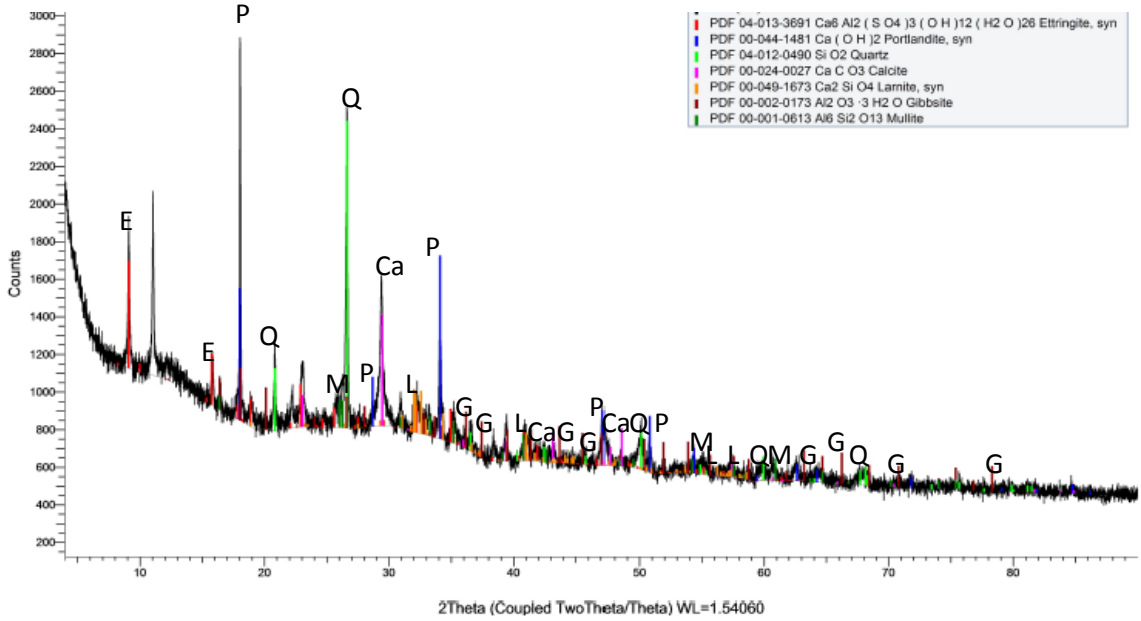

Figure 9(b) Mix 10-F1 (60% Fly ash 1+ 30% CEM 1 + 10% CKD) [Ca=Calcite, E=Ettringite, G=Gibbsite, L=Larnite, M=Mulite, P=Portlandite, Q=Quartz]

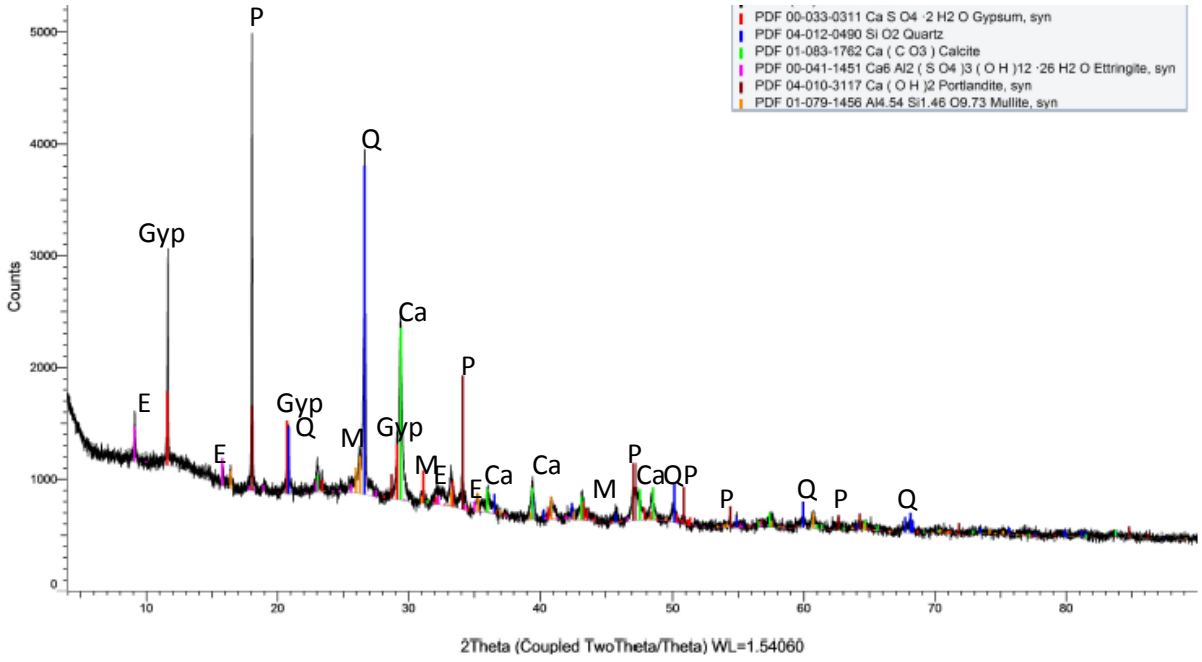

Figure 9(c) Mix 11-F1 (60% Fly ash 1 + 30% CEM 1 + 10% Gypsum) [Ca=Calcite, E=Ettringite, Gyp=Gypsum, M=Mulite, P=Portlandite, Q=Quartz]

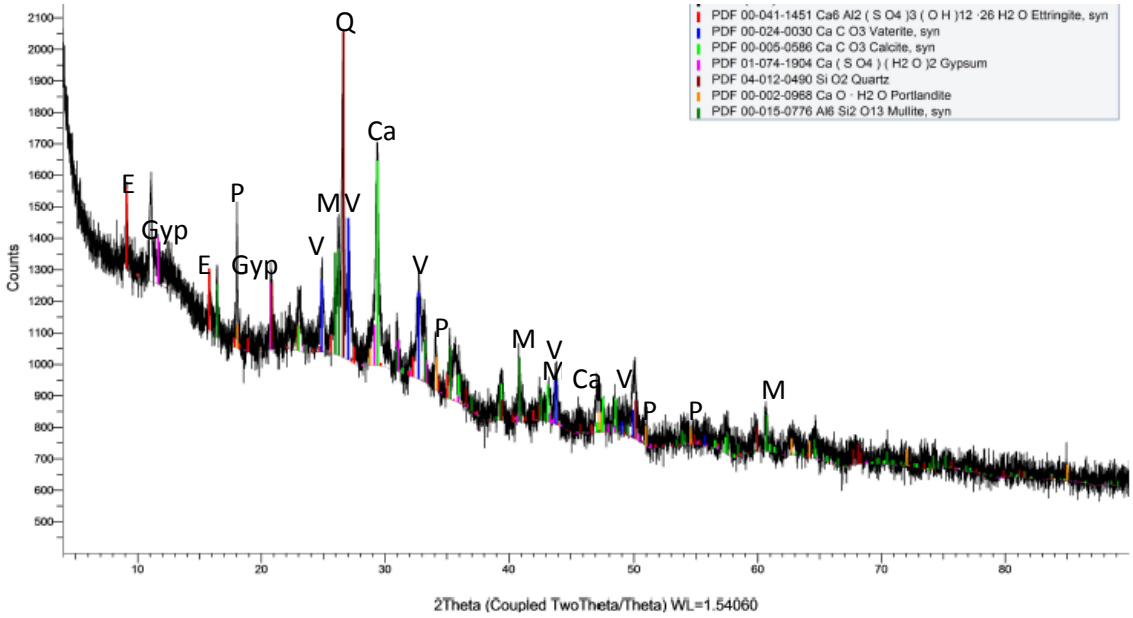

Figure 9(d) Mix 1-F2 (70% Fly ash 2+ 30% CEM 1) [Ca=Calcite, E=Ettringite, Gyp=Gypsum, M=Mulite, P=Portlandite, Q=Quartz, V=Vaterite]

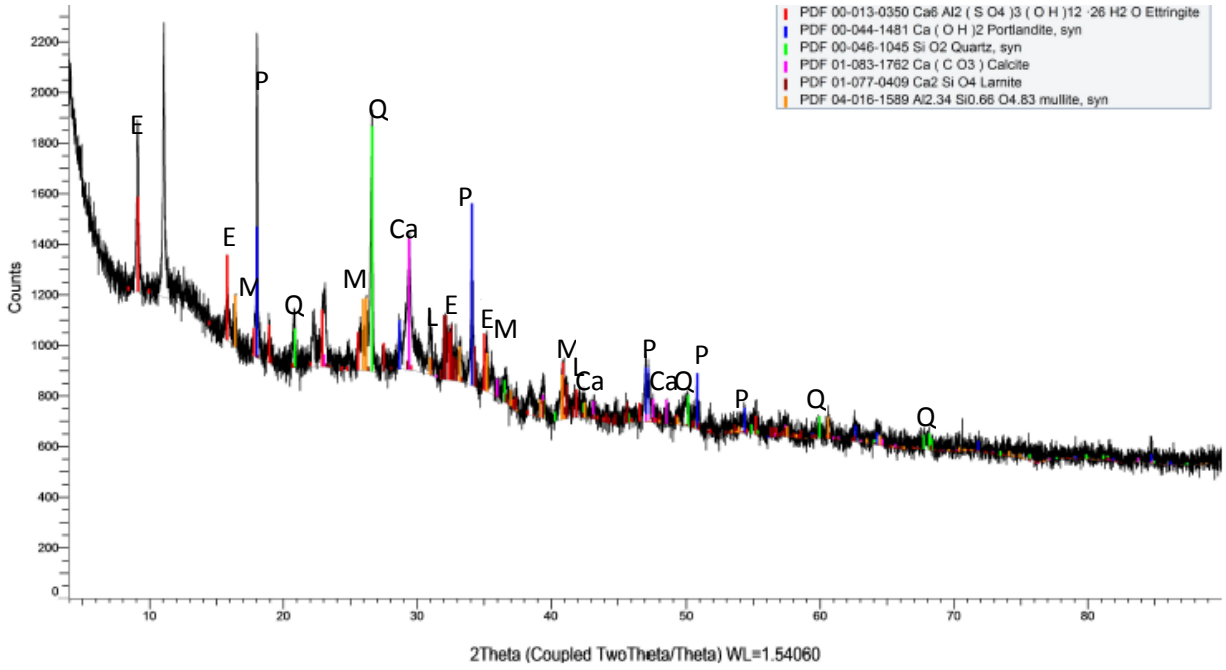

Figure 9(e) Mix 10-F2 (60% Fly ash 2+ 30% CEM 1 + 10% CKD) [Ca=Calcite, E=Ettringite, Gyp=Gypsum, L=Larnite, M=Mulite, P=Portlandite, Q=Quartz]

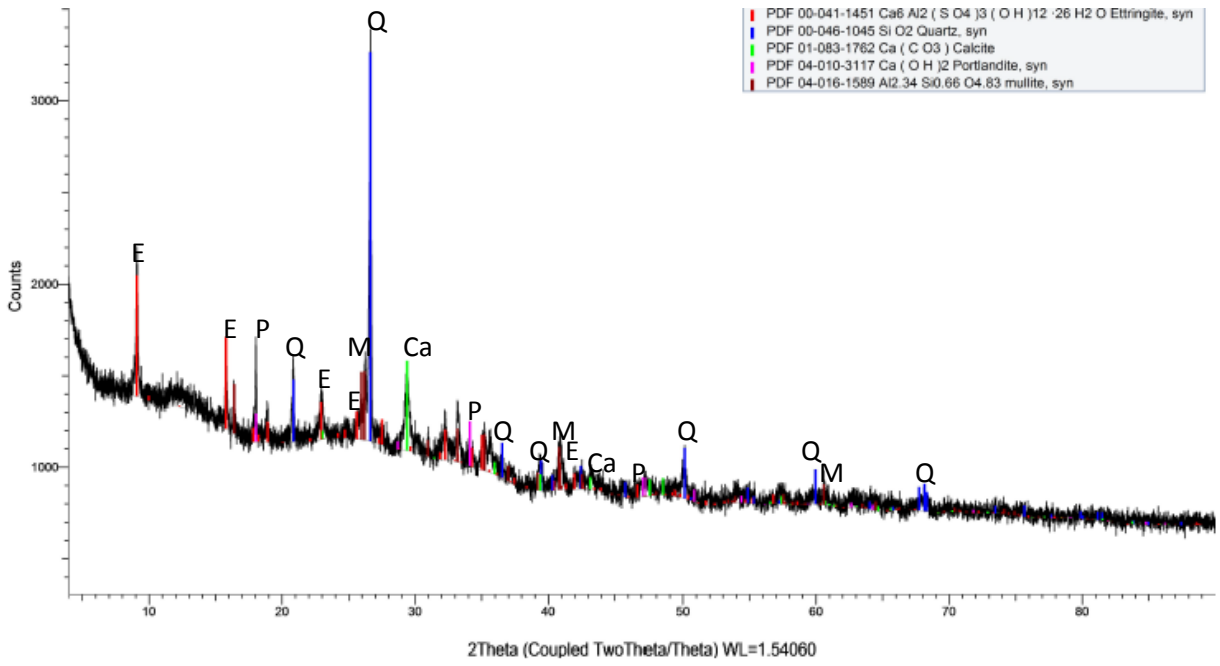

Figure 9(f) Mix 11-F2 (60% Fly ash 2 + 30% CEM 1 + 10% Gypsum) [Ca=Calcite, E=Ettringite, M=Mulite, P=Portlandite, Q=Quartz]